E2F7 and E2F8, as Potential Mediators of Rb, are Essential for Cell Survival and Embryonic Development

A Senior Honors Thesis

Presented in partial fulfillment of the requirements for graduation with distinction in Molecular Genetics in the College of Biological Sciences of The Ohio State University

By

Cong Ran

The Ohio State University

June 2007

Project Advisor: Dr. Gustavo Leone, Department of Molecular Virology, Immunology, and Medical Genetics

Abstract:

E2f transcription family encompasses a wide-range of functions in regulating cell proliferation, cell differentiation and apoptosis. The two recent additions to the E2F family, *E2f7* and *E2f8*, had unique structural features that set them apart from E2Fs. These structural features enabled these two E2Fs with the capacity for homo-dimerization and hetero-dimerization, and hence they can redundantly regulate downstream target like *E2f1* and *p53*. Unlike the function of other E2F members, E2F7 and E2F8's biological function in mouse development was found crucial. Simultaneous deletion of *E2f7* and *E2f8* induces ectopic E2F1-P53 dependent apoptosis in addition to vascular formation defect and placental deformation that eventually lead to early embryonic lethality at E11.5. My work strongly suggests that functions of E2F7 and E2F8 in the extra-embryonic cell lineages are vital for embryos to survive until term. I here show that preserving functional E2F7 and E2F8 in placental tissue allows fetuses deficient for *E2f7* and *E2f8* go to term, but these animals were still physiologically impaired and died soon after birth. The phenotype stemming from losses of *E2f7* and *E2f8* in mouse development mimicked that resulted from the loss of Rb, indicating that E2F7 and E2F8 can potentially mediate Rb in regulating cell-cycle progression and apoptosis during development and potentially during tumorgenesis.

Introduction:

The Retinoblastoma (Rb) gene was identified twenty years ago as the first tumor suppressor. It was initially identified by positional cloning due to its frequent loss-of-function mutation

found in pediatric eye tumors. Aberrant signaling pathways and direct mutations of the Rb gene have been since linked to various tumorgenic processes in wild-ranges of tissue types (Harbour and Dean, 2007). Besides its obvious function as a tumor suppressor, Rb's biological function is required in mouse development. The ablation of Rb in mice induces abnormal cellular activities and severe physiological defects that lead to embryonic lethality at E14.5. Loss of Rb induced unscheduled trophoblast cell proliferation and destruction of placental labyrinth architecture that disrupts normal maternal-fetal transportation. Furthermore, neurogenic defects were discovered in embryos lacking Rb. These mutant embryos had massive ectopic cell cycle entry and elevated apoptosis in central nervous system and peripheral nervous system (Wenzel et al, 2007, de Bruin A. et al, 2003). During embryonic developmental stages, Rb function was seen exceptionally important in the extra-embryonic compartment; deletion of Rb in these tissues alone was capable of inducing embryonic death (Wenzel et al, 2007, de Bruin A. et al, 2003).

The Rb gene product, pRb, is a nuclear phosphoprotein that arrests cell cycle at the G1/S transition. The tumor suppression function of Rb requires the central "pocket" domain that was most naturally targeted in tumor-promoting events. Sequences within such domain are required for the binding of Rb with endogenous proteins that regulate cell-cycle progression (Grana et al, 1998). During cell cycle, three different cyclin and cyclin-dependent kinase (cdk) complexes activate Rb signaling pathways by phosphorylation at specific sites of Rb. Rb can also command cell cycle repression as an effector of cdk inhibitor and p53 (Harbour and Dean, 2007).

In the Rb paradigm that has emerged in the last twenty years since its discovery, a family of transcription factors, the E2f transcription factors appeared to be an important group of downstream effectors, *in vitro* evidence has suggested that each performing distinct functions in regulating normal and tumorgenic cellular activities. Phosphorylation of Rb during cell cycle

can release E2Fs from the Rb-E2F complexes to promote E2F-dependent transcriptions and subsequent cell-cycle progression (Harbour and Dean, 2007). The complexity of the Rb-E2f model was not restricted to the cell-cycle related regulation of Rb, since constitutive expression of Rb and its pocket proteins p130 and p107 recruits several E2fs and corepressors such as chromatin remodeling complexes to elicit multiple molecular responses which repress cell-proliferation (Grana et al, 1998).

A large body of work suggests that E2Fs can function to activate and repress the transcription of many essential genes involved in cell proliferation, apoptosis and differentiation (Dimova, Dyson 2005). The fact that E2F activity can be regulated during the cell cycle at multiple levels, including by direct binding of the Rb tumor suppressor, as well as by transcription, protein degradation and post-translational mechanisms suggests that cell cycle-dependent regulation of E2F is critical for cellular homeostasis. The effects of deregulated E2F activity are pleiotropic and vary in different experimental settings, either promoting cellular proliferation or cell death. While a decrease in E2F activity is associated with a reduction in the proliferation capacity of cells, an increase in E2F activity is often associated with the induction of apoptosis. Depending on the tissue examined, E2F-induced apoptosis can be p53-dependent or independent. More recent studies have begun to reveal specific roles of E2F family members in the control of proliferation and apoptosis.

The mammalian E2F proteins are encoded by eight distinct genes (E2F1-8) and are believed to play a critical role in orchestrating the oscillatory pattern of cell cycle dependent gene expression. Based on structure-function studies and amino acid sequence bioinformatics analysis, the E2F family can be conveniently divided into two general subclasses, transcription repressors and activators. The repressor subclass consists of E2F3b, E2F4, E2F5, E2F6, E2F7

and E2F8. With the exception of E2F7 and E2F8, this group is constitutively expressed during the cell cycle and serve to recruit Rb- related pocket proteins and a number of associated co-repressor proteins to E2F-target promoters, resulting in their repression during G_0 (Attwooll et al., 2004). As cells are stimulated to enter the cell cycle, cyclin dependent kinases phosphorylate pocket proteins, leading to the dissociation of E2F repressor complexes and the derepression of E2F-target genes. The activator subclass, consisting of E2F1, E2F2 and E2F3a, are themselves repressed by E2F repressor complexes. Thus, cdk-dependent phosphorylation of pocket proteins leads to the accumulation of E2F1, E2F2 and E2F3a proteins late in G_1. These activators then transiently bind to E2F-binding elements on target promoters, resulting in their acute activation at the G_1/S transition. Consistent with an important function in regulating gene expression during G_1/S, the over-expression of activators in quiescent cells can potently transactivate many of these G_1/S regulated E2F-responsive genes. The consequence of this regulation to cell proliferation was highlighted by the analysis of mouse embryonic fibroblasts (MEFs) deficient for E2F1, E2F2, and E2F3. In these experiments, the acute loss of the three activator E2Fs resulted in a reduction of E2F target genes and a severe block in cell proliferation (Wu 2001). While a great deal is now understood about how E2F3b/4/5/6-mediated repression in G_0 is coordinated with E2F1/2/3a-mediated activation in G_1/S to regulate the induction of E2F targets as cells enter the cell cycle, little is known about how target genes are subsequently downregulated during S/G_2 to complete the oscillation of gene expression observed during the cell cycle.

E2F7 and E2F8 have unique features among the E2F family. These novel E2Fs lack the leucine-zipper domain required for dimerization with the partner proteins DP1/2 (Figure 1). In addition, E2F7 and E2F8 possess two DNA binding domains that allow them to function in a

DP-independent manner. The two separate domains exhibit high homology to the DNA binding domains of E2F, both of which are essential in binding to *E2f* DNA consensus sequences. In contrast to the rest of the E2F family, E2F7 and E2F8 are maximally expressed during S and G_2 phases of the cell cycle. Together with their ability to repress gene expression and block cell proliferation in cultured cells, these observations suggest that E2F7 and E2F8 may represent as a unique arm of the E2F network.

To investigate the physiological functions of E2F7 and E2F8 *in vivo*, the Leone Lab has used homologous recombination techniques to target the inactivation of *E2f7* and *E2f8* in mice. I found that while single deletion has no effect on mouse development, the combined loss of *E2f7* or *E2f8* results in the accumulation of E2F1 and p53, massive apoptosis throughout fetal tissues, and embryonic lethality by E11.5. The execution of apoptosis in *E2f7*$^{-/-}$*E2f8*$^{-/-}$ embryos was found to be E2F1 and p53 dependent. These data define a role for E2F7 and E2F8 in embryonic cell survival via direct control of the E2F1-p53 axis. While removing downstream effectors *E2f1* or *p53* can relieve aberrant apoptosis in *E2f7*$^{-/-}$*E2f8*$^{-/-}$ embryos, it cannot halt embryonic lethality caused by simultaneous loss of *E2f7* and *E2f8*. Surprisingly, only reconstitution of mutant fetuses with normal wild-type placentas can restore normal gestation, indicating that disruption *E2f7* and *E2f8* have deleterious consequences in placental development and embryo survival.

Materials and methods

Generation of *E2f7* and *E2f8* knockout mice

PCR generated probes for *E2F7* and *E2F8* were used to screen a 129Sv/Ev bacterial artificial chromosome library. A 7-kb XbaI fragment of *E2F7* spanning exon 4 and 5 was isolated from *RPCI 22 431 H17* and a 6.64-kb fragment of *E2F8* containing exon 3 and 4 was isolated from

RPCI 22 539 P23. To generate *E2F7* and *E2F8* targeting constructs, both fragments were first subcloned into pBluescript and subsequently engineered into pLoxPII (ref.) with flanking *loxP* sites and a neomycin cassette inserted in reverse orientation. The pLoxPII targeting vector was linearized with NotI, and electroporated into TC1 129Sv/Ev embryonic stem (ES) cells (ref). Cells undergoing homologous recombination were selected by growth on G418 plus ganciclovir and verified by Southern blot using indicated probes. Selected ES clones were injected into C57BL/6 blastocysts to generate chimaeric mice. I bred the resulting chimaeric males with National Institute of Health (NIH) Black Swiss females to achieve germline transmission. Offspring were bred to *EIIa-Cre* mice to excise the neomycin cassette to produce conventional and conditional null mice. Genotypic analysis of offspring was performed by Southern blot analysis and multiplex PCR using three primers: E2F7-a, 5'-AGGCAGCACACTTGACACG-3'; E2F7-b, 5'-ACTTTTGGGACAGAGGTAGGA-3'; E2F7-c, 5'-CCAAGATGAAGGCCGAGATGCTAC-3'; or E2F8-a, 5'-TAAAAAGCTTTGCGGTCGTT-3'; E2F8-b, 5'-AAGCCAACCTCGATGAATTG-3'; E2F8-c, 5'-CTCGCATCATCGTCTGCTAA-3').

Quantitative real-time PCR

Total RNA was isolated using Qiagen RNA miniprep columns as described by the manufacturer, including the optional DNase treatment before elution from the column. Reverse transcription of total RNA was performed using Superscript III reverse transcript reagents (Invitrogen) and RNAse Inhibitor (Roche) according to the manufacturer's instruction. Real-time RT-PCR was performed using the BioRad iCycler PCR machine. Reactions were done in triplicate and relative amounts of cDNA were normalized to GAPDH. Primer sequences are available upon request.

Co-immunoprecipitation assay

Human embryonic kidney HEK293 cells were cultured in DMEM medium supplemented with 15% FBS and used for co-immunoprecipitation assay. Transient transfections with indicated constructs were performed by standard calcium chloride technique. Transiently transfected HEK293 cells were harvested in cold phosphate-buffered saline, and cell pelletes were lysed in 10 times volume of lysis buffer (0.05M sodium phosphate PH7.3, 0.3M NaCl, 0.1% NP40, 10% glycerol with protease inhibitor cocktail). Co-immunoprecipitation was performed as described. For analysis of protein interactions, Flag and/or HA tagged proteins were transfected as indicated in Figure 5. Flag or HA antibody was used for the precipitation. After extensive washing, proteins bound to affinity resins were resolved by SDS-PAGE and detected by Western blotting as indicated.

Immuno-affinity Purification (IAP)

E2F7 associated complexes were purified from Hela cells stably transduced with FLAG-HA tagged E2F7 (ref). Nuclear extracts were prepared by modified Dignam prep in that nuclei pellets were extracted with Buffer C-450 (20mM HEPES, pH 7.9, 450 mM KCl, 1.5 mM MgCl2, 25% glycerol, 0.2mM EDTA) equal to the nuclei pellet volume (ref). Resulting extracts were incubated with pre-equilibrated FLAG M2 affinity resin (Sigma) for 3h. Resin/extract mixtures were decanted onto Bio-Spin columns (BioRad) and allowed to empty by gravity. After 3 washes with 10 column volumes of Wash Buffer (20mM HEPES, pH 7.9; 150mM KCl; 10% glycerol; 0.2mM EDTA), complexes were eluted by incubation with Wash Buffer plus

200μg/mL of FLAG peptide (Sigma) for 1h, followed by a brief spin to collect the eluents. The FLAG eluents were subsequently subjected to Western blot analysis using anti-E2F8 antibody. All nuclear extraction and immuno-affinity purification steps were done at 4˚C and fresh protease inhibitors were added to all working solutions. . Hela cells were transduced with retroviruses expressing a bicistronic mRNA encoding human E2F7 (Flag-HA-7) linked to an interleukin-2 receptor (IL-2R)-α as surface marker. The transduced subpopulation was purified by affinity sorting (S). Cells before and after sorting

Chromatin immunoprecipitation (ChIP) and sequential ChIP assays

For ChIP assay, the EZ CHIP^{TM} assay kit (Upstate Biotech) was used as described by the manufacturer. Briefly, harvested HEK293 cells overexpressing E2F7 and/or E2F8 were cross-linked and chromatin was sonicated to an average size of 200-1000bp. Lysates were subsequently pre-cleared with Salmon Sperm DNA/Protein G agarose slurry (Upstate). Then antibodies specific to Flag, HA, or normal mouse IgG (Oncogene) were added to each sample and incubated overnight at 4^{o} C. Antibody-protein-DNA complexes were recovered by addition of 30 μl of Salmon Sperm DNA/Protein G agarose slurry and incubation for 1 hour at 4^{o} C. Following extensive washing, the complexes were eluted and cross links were reversed by heating the samples to 65^{o} C for 4 hours. Finally, samples were treated with Proteinase K (Roche) and Rnase A (Roche) and purified through Qiaquick columns (Qiagen). Real-time PCR was performed using the Biorad iCycler PCR machine with the specific primers of certain promoter regions. Reactions were done in triplicate and normalized using the threshold cycle number for the total input sample.

Sequential ChIP-PCR was carried out using the same EZ CHIP™ protocol, except involving two rounds of chromatin immunoprecipitation steps. The first round of immunoprecipitation was performed by incubation with M2 anti-FLAG antibody and Salmon Sperm DNA/Protein G agarose slurry. Precipitated DNA-protein complexes were eluted by 1h incubation with Flag peptide (F3290, Sigma) at 4°C and then subjected to a second round of precipitation with primary antibodies as indicated in Figure 6c. After extensive washing, sequentially precipitated complexes were recovered by addition of 30 μl of Salmon Sperm DNA/Protein G agarose slurry and incubation for another 1h at 4° C. Protein-DNA complexes collected from Sequential ChIP were treated and subjected to the real-time PCR analysis as described above for ChIP experiments. Primer sequences are available upon request.

Western blot and antibodies

Immunoblotting analyses were done by standard procedure. The following commercial antibodies were used as indicated in the figures: Caspase-3 (9662, Cell Signaling), p53 (Ab-1, Oncogene), E2F1 (C-20, Santa Cruz), Flag (M2, Sigma), E2F8 (M01, Abnova), HA (12C5A, Rocha), Myc (9E10, Santa Cruz). Primary antibody blotting was detected using appropriated horseradish-peroxidase-conjugated secondary antibodies and ECL reagent as described by the manufacturer (Amersham Biosciences).

FACS analysis

E2F7/8 knockout MEFs were synchronized by starvation in DMEM containing 0.2% FBS for 48h and blocked at the G1/S transition by the addition of DMEM containing 15% FBS and 1mM hydroxyurea (HU) for 18h. Cells were then washed 3 times with PBS and released into the cell

cycle by adding fresh medium containing 15% FBS. Cells were harvested at the indicated time points and processed for flow cytometry, quantitive real-time PCR. For FACS analysis cells were harvested by trypsinization, fixed in 70% ethanol and stained with propidium iodide using standard protocol.

Cell culture, proliferation and viability assay

E2F7 and E2F8 conditional knockout mouse embryonic fibroblasts (MEFs) were isolated from E13.5 embryos and maintained in DMEM medium containing 12.5% fetal bovine serum (FBS). Immortalized cell lines were generated from primary MEFs using standard 3T3 and 3T9 protocol. To obtain conventional DKO cells, I transfected immortalized MEFs with retrovirus expressing Cre recombinase using standard methods (ref.).

Cell Growth Measurement

To measure the proliferation rate of MEFs, $1x10^{\wedge 6}$ cells were seeded to 10mm cell culture dish (Corning) on the initial day of experiment. Each following 24 hours, total cell numbers were assayed by trypan blue exclusion method, and all cells were re-seeded for similar analysis at succeeding time-points.

BrdU and TUNEL asssays

Pregnant females at 9.5 days postcoitum were injected intraperitoneally with BrdU (100 ug/grams of body weight) 3 hours prior to harvesting. Embryos were fixed in formalin upon harvesting and 5um paraffin embedded-sections were used for immunohistochemistry analysis after deparaffinization. Anti-BrdU antibody (DAKO Co. MO-0744) and Vectastain Elite ABC

reagent (Vector labs) were used to detect BrdU incorporation according to the manufacturer's instructions, followed by hematoxylin counterstaining. Apoptotic cells were determined using TUNEL assay (Chemican S7101), according to the manufacturer's protocol. All slides were counterstained with hematoxylin. Proliferation and apoptosis were measured by quantitation of the ratio between positive-signaling and total cells.

Tissue processing and β-galactosidase staining assay

Tissue was excised and portions were processed for *in situ* X-gal staining. Tissue was fixed directly in paraformaldehyde (2% PFA/0.2% glutaraldehyde in a 100 mM sodium phosphate buffer, pH=7.4) for 2 to 2.5 hours at 4^{o}C, washed for 10 min twice in phosphate-buffered saline (PBS) and then stained in a 5-bromo-4-chloro-3-indolyl-D-galactopyranoside (β-gal) solution [4 mM potassium ferricyanide (Sigma), 4mM potassium ferrocyanide (Sigma), 2 mM magnesium chloride (Sigma), 0.2% IGEPAL CA-630 (NP-40 substitute, Sigma), 0.1% sodium deoxycholic acid (Calbiochem) and 1 mg/mL β-gal (Gold Bio Technology, St. Louis, MO) in PBS for 18 hours at RT protected from light. β -gal-stained tissue was washed for 10 min twice with PBS and post-fixed in 10% neutral-buffered formalin (Richard Allen) for 48 hrs at RT.

Results

E2F7 and E2F8 are essential for embryonic viability

To investigate E2F7 and E2F8 functions *in vivo,* the Leone lab utilized cre-*loxP* technology to disrupt E2F7 and E2F8 function in mice. Targeting of *E2f7*and *E2f8* was achieved by flanking exon 4 in *E2f7* and exon 3 and 4 in *E2f8* with *loxP* sites using homologous recombination

techniques (Figure 2a). In each case, exon 4 encodes essential sequences for specific DNA binding activity and ablation of *loxP*-flanked sequences is predicted to result in a shift of the open reading frames, leading to premature termination of translation. Correct targeting of *E2f7* and *E2f8* in ES cells was verified by Southern blot and PCR analysis (data not shown). Correctly targeted ES clones were injected into C57BL/6 blastocysts and chimeric male mice were mated with Black Swiss females. Agouti offspring with germline transmission of the targeted alleles were then bred with *EIIA-cre* mice. Pups lacking either the neo cassette (conditional knockout alleles; $E2f7^{loxP/+}$ and $E2f8^{loxP/+}$) or both the neo cassette and the *loxP*-flanked regions of *E2f7* or *E2f8* (conventional knockout alleles; $E2f7^{+/-}$ and $E2f8^{+/-}$) were identified by Southern blot and PCR genotyping analysis (Figure 2b).

Intercrosses between $E2f7^{+/-}$ or $E2f8^{+/-}$ animals resulted in viable $E2f7^{-/-}$ and $E2f8^{-/-}$ offspring that appeared externally normal, were fertile and lived to old age. Given the structural and functional similarities between E2F7 and E2F8 (ref), I investigated the possibility that these family members could compensate for the absence of the other. Real-time PCR analysis of *E2f7* and *E2f8* expression, however, revealed that their expression was unperturbed in single knockout embryos (Fig. 2c) or mouse embryo fibroblasts derived from embryos (data not shown), suggesting that compensation between these family members was not taking place in these animals, at least at the mRNA level. To explore the possibility of functional redundancy between E2F7 and E2F8 I examined the biological consequence of ablating both. To this end, I intercrossed $E2f7^{+/-}E2f8^{+/-}$, $E2f7^{-/-}E2f8^{+/-}$ and $E2f7^{+/-}E2f8^{-/-}$ animals and analyzed the resulting offspring. Whereas $E2f7^{-/-}E2f8^{+/-}$ and $E2f7^{+/-}E2f8^{-/-}$ pups were found at the expected Mendelian ratios, no $E2f7^{-/-}E2f8^{-/-}$ double knockout (DKO) pups were found at birth (P0). Analysis at

earlier stages of embryonic development revealed that only 50% of the DKO embryos were alive at embryonic day 10.5 (E10.5), and no DKO embryos were alive at E11.5 (Table 1).

E2F7 and E2F8 form homo- and hetero-dimers

Previous studies demonstrated an ability of E2F7 and E2F8 to form homodimers (Figure 3a, top panels; ref). The fact that E2F7 and E2F8 are coexpressed in most cells of the embryo and appear to have overlapping functions *in vivo* led me to explore the possibility that E2F7 may physically interact with E2F8. Because immunoprecipitation-quality antibodies for E2F7 and E2F8 are not yet available, my mentor Jing Li used HeLa cells expressing flag-hemagglutinin (HA) epitope tagged E2F7 to assess whether endogenous E2F8 could be found in complex with the doubly-tagged version of E2F7. As shown in Figure 3b, sequential immunoprecipitations with anti- flag and anti- HA antibodies revealed a specific interaction between endogenous E2F8 and flag-HA-E2F7. Similarly, endogenous E2F7 could be found in association with flag-HA-E2F8 (data not shown). The interaction between E2F7 and E2F8 was confirmed by co-immunoprecipitation assays using HK293 cells co-expressing flag-tagged E2F7 and HA-tagged E2F8 (Figure 3a).

Given that E2F7 and E2F8 can form homodimers as well as heterodimers, I evaluated the preferred dimerization state in cells. To this end, cells were co-transfected with flag-7, HA-7, and myc-8 or with flag-8, HA-7, and myc-8, and flag-immunoprecipitates were blotted with either anti-HA or anti-myc. The immunoprecipitated E2F7 or E2F8 was quantified relative to 1% of the input material. As shown in Figure 3c, E2F7 had a greater binding affinity to itself than to E2F8. On the other hand, E2F8 had a greater affinity for E2F7. From this analysis I conclude that the preferred state of dimerization is E2F7:E2F7 > E2F7:E2F8 > E2F8:E2F8.

E2f1 is a direct target of E2F7 and E2F8

Chromatin immunoprecipitation (ChIP) assays were then used to assess the ability of E2F7 and E2F8 to bind known E2F target promoters. HEK293 cells transiently transfected with a flag-tagged E2F7 or E2F8 were cross-linked with formaldehyde, extracts were prepared, DNA was fragmented and the chromatin material was immunoprecipitated with antibodies specific for the flag epitope. Quantitative real-time PCR assays designed to measure the enrichment of *E2f1* promoter or control *tubulin* promoter sequences in immunoprecipitated DNA show that E2F7 is specifically recruited to E2F binding sites on the *E2f1* promoter (Figure 4d). This recruitment was specific since IgG immunoprecipitates or anti-flag immunoprecipitates of flag-E2F7 DBD1 mutant extracts failed to specifically amplify *E2f1* promoter sequences. Similarly, E2F8 could be specifically recruited to the *E2f1* promoter (data not shown).

I then addressed whether E2F7-E2F8 heterodimers could bind the *E2f1* promoter. To this end, HEK293 cells expressing HA-tagged E2F7 and Flag-tagged E2F8 were first immunoprecipitated with anti-flag antibody; immunopreciptated DNA-protein complexes were then eluted with excess flag peptide and reimmunoprecipitated with HA-specific antibodies. The final immunoprecipiates were then similarly amplified with primers specific for the *E2f1* or *tubulin* promoters. These sequential ChIP assays show that E2F7 and E2F8 simultaneously occupy E2F binding sites on the *E2f1* promoter (Figure 3e). From these experiments, I conclude that E2F7 and E2F8 homodimers and heterodimers can be specifically recruited to the *E2f1* promoter.

E2f1 expression is derepressed in *E2f7*$^{-/-}$*E2f8*$^{-/-}$ MEFs.

To determine whether the recruitment of E2F7 and E2F8 to the *E2f1* promoter has a functional consequence on its expression, I examined E2F1 protein and mRNA levels in *E2f7*$^{-/-}$*E2f8*$^{-/-}$ MEFs. Western blot and real-time PCR assays showed a consistent increase of E2F1 protein and mRNA levels in DKO MEFs relative to *wild type* MEFs (Figure 4b and 4c), suggesting that E2F7 and E2F8 are required for the repression of *E2f1*. This increase in *E2f1* expression is likely due to transcriptional deregulation of its promoter since *E2f1* luciferase promoter activity was similarly elevated in DKO cells. Importantly, mutation of the E2F and CRH binding elements on the *E2f1* promoter resulted in a derepression of reporter activity in *wild type* but in DKO MEFs (Figure 4d), suggesting that the regulation of *E2f1* expression by E2F7 and E2F8 is direct.

E2f7 and *E2f8* expression fluctuates during the cell cycle, with maximal expression in S and G_2; I hence evaluated *E2f1* expression in DKO MEFs more closely at various stages of cell cycle progression. To this end, *wild type* and DKO MEFs were synchronized by serum deprivation, followed by restimulation with medium containing 10% serum and 2mM hydroxyurea (HU). Cells synchronized at G_1/S were stimulated to enter S phase and to progress though the cell cycle by removing HU from the medium. Cell cycle progression was monitored by flow cytometry (Figure 4e). Cells harvested periodically were processed for RNA and protein and *E2f1* expression at each time point was evaluated by real-time PCR and Western blot assays. As expected, *E2f1* expression in *wild type* cells accumulated during G_1/S and subsequently decreased during S and G_2. Strikingly, expression of *E2f1* in DKO cells continued to increase as cells progressed through S and G_2, accumulating upto 12-fold higher than in *wild type* cells (Figure 4f). These data suggest an important role for E2F7 and E2F8 in repressing E2F-target expression during S and G_2 phases of the cell cycle.

E2f7$^{-/-}$*E2f8*$^{-/-}$ DKO cells proliferate normally but are hypersensitive to apoptosis *in vitro*

Given the fact that *E2f1* is unregulated in the *E2F7*$^{-/-}$*;E2F8*$^{-/-}$ DKO cells and overexpression of E2F1 will lead to proliferation and apoptosis, I examined the effect of loss of E2F7 and E2F8 on proliferation and apoptosis using mouse embryonic fibroblasts (MEFs). Since conventional *E2F7*$^{-/-}$*;E2F8*$^{-/-}$ DKO embryos die during early mouse development, MEFs were isolated from conditional embryos at E13.5, and deletion of the floxed alleles was performed *in vitro* by infection with a retrovirus expressing the Cre recombinase. Proliferation index of E2F7/8 primary MEFs was evaluated by performing the growth curve assay (Figure 5a). Detailed analyses of the in vitro proliferation rates revealed that the proliferation of *E2f7*$^{-/-}$*E2f8*$^{-/-}$ cells were not impaired compared with wild type controls.

To evaluate the apoptosis index, DKO were exposed to the DNA damaging drugs camptothecin and cisplatin. Asynchronously proliferating wild type and conditional deleted DKO MEFs were treated for 18h with camptocethin. The viability of the treated cells was determined by trypan blue exclusion at different time intervals post treatment. I found that camptocethin induced a significant acceleration of cell death in DKO MEFs compared to wild type MEFs (Figure 5b and 5c). Furthermore, treatment with cisplatin triggered cleavage of Caspases-3 in *E2f7*$^{-/-}$*E2f8*$^{-/-}$ MEFs, evaluated by Western blot analysis (Figure 5d). These data indicate that loss of E2F7 and E2F8 results in increase sensitivity towards apoptosis *in vitro.*

Depending on the cell type analyzed, the induction of apoptosis by deregulated E2F may be p53-dependent or independent (reviewed in Trimarchi and Lees, 2002; Bell and Ryan, 2004) Previous studies have shown that *E2f1* can induce apoptosis in p53-dependent and p53-independent manner. To further explore the mechanism of apoptosis triggered by the absence of E2F7 and E2F8, I confirmed the deregulation of E2F1 and p53 expression by Western blot

analysis (Figure 5e) and evaluated the expression of p53 target genes by real-time RT-PCR (Figure 5f). DKO MEFs showed a marked increased expression of p53 targets compared to wild type cells. Following camptocethin treatment, the levels of gene expression accelerated, in particular the levels of the p53 target genes, *gadd45* and *noxa* were strongly elevated in DKO MEFS. Taken together these findings suggest that E2F7 and E2F8 repress apoptosis by inhibiting the E2F1-p53 signaling pathway.

Concomitant ablation of *E2f7* and *E2f8 in vivo* has no effect on proliferation but induces E2F1-p53 dependent apoptosis

Having *in vitro* data, the next question was whether the same phenotype will be observed *in vivo* under normal physiological conditions. To assess whether loss of *E2f7* and *E2f8* influenced the level of proliferation occurring *in vivo*, I injected BrdU into pregnant females (1 or 3 hours before sacrifice) and measured BrdU incorporation immnunohistologically in serial sections. As the representative pictures shown in Figure 8, there is no dramatic difference observed between DKO and wild type embryos.

In contrast to our analysis of proliferation, I easily noticed comultifocal areas with abundant pyknotic and karyorrhectic nuclei which were present within the mesoderm, the branchial arch, the somites and the neural tube of DKO fetuses. Consistently with these findings, these regions were preferentially labeled by the TdT-mediated dUTP nick end-labelling (TUNEL) assays, indicative of inappropriate apoptosis. The frequency of apoptosis was three to five fold greater in DKO fetuses than in control siblings (Figure 7c).

Based on the facts that induction of E2f1 and p53 was observed in *E2f7*$^{-/-}$*E2f8*$^{-/-}$ *MEFs,* which are components previously associated with hypersensivity of cell death. The hypothesis

then was that loss of *E2f7* and *E2f8* could lead to increase of apoptosis in an E2F1-p53 dependent manner. To test this hypothesis, I bred animals to either E2F1 or p53 mutant background. If the massive apoptosis of the 78-deficient embryos were due to over expression of E2f1 and p53, the inactivation of E2f1 and p53 could reduce this apoptosis. Analysis of $E2f7^{+/-}$ $E2f8^{+/-}E2f1^{-/-}$ or $E2F7^{+/-}E2f8^{+/-}p53^{-/-}$ embryos from triple mutant crosses revealed that inactivation of E2f1 or p53 clearly rescued the apoptosis phenotype of DKO embryos to normal status (Figure 7c). However, these embryos still died at similar stage of gestation time like E2F7 and E2F8 deficient embryos.

E2F7 and E2F8 are required for angiogenesis

To evaluate the possible cause of the intrauterine death of $EfF7^{-/-}E2f8^{-/-}$ animals, I analyzed of haematoxylin- and eosin-stained sections obtained from wild-type and $E2f7^{-/-}E2f8^{-/-}$ deficient placentas. Normally at around embryonic day 9-10, the allontois attaches to the chorionic plate, which is the initial step in the formation of a functional placenta, followed by vascular invasion of the labyrinth layer. The labyrinth is the site of oxygen and nutrient exchange between the mother and fetus, and consists of highly branched, trophoblast-covered maternal blood sinusoids in direct contact with the underlying fetal blood vessels. The wild-type labyrinth therefore has a porous appearance, with trophoblast cells being well organized and distributed around fetal and maternal blood vessels (Figure 9a). The fetal blood vessels contain nucleated erythrocytes invade and interdigitate into the labyrinth layer of the developing placenta.

Placentas of viable DKO mutants were of normal size; however fetal blood vessels remain at the chorionic plate and did not efficiently invade into the labyrinth layer (Figure 9a). Maternal sinuses, containing mature nonnucleated erythrocytes, could be however readily

observed in the labyrinth. Vascular defects were also observed in the yolk sacs and in the embryo proper, characterized by large dilated and disorganized blood vessels with reduced branching of the vascular tree (Figure 9b). In addition starting at day E10.5, there was fluid extravasation in the pericardial cavity, as well as hemorrhages in the pericardium and the placenta of DKO animals. These findings suggest a defect in vascular differentiation with impaired angiogenic sprouting and remodeling in DKO mutants. These observations, however, will need to be confirmed by further analysis.

Extra-embryonic function of E2F7 and E2F8 are essential for embryonic viability

The physiological defects observed in *E2f7-8* deficient animals had led me to examine the biological significance of *E2f7* and *E2f8* presence in placenta. Harnessing the advantages of Cre-loxp transgenic system, I was able to selectively disrupt *E2f7* and *E2f8* in specific cell lineages. I utilized $E2f7^{loxP\ /loxP}E2f8^{loxP\ /loxP}$ conditional knockout mice and $Sox2^{+/cre}$ transgenic mice to reconstitute E2f7-8 deficient embryos with a functionally 'wild-type' placenta. Previous studies had proven that using Cre-recombinase controlled by endogeneous Sox-2 promoter is sufficient to deliver functionally active Cre expression in all cells of embryo proper at E6.5 while producing little expression in the extra-embryonic compartment. B-galactosidase staining of E12.5 and P0 animals including placenta derived from $Sox2^{+/cre}$ and $Rosa26^{loxP/loxP}$ reporter mice interbreedings verified the specific expression of Cre in fetal tissues as previously reported (Figure 10a)

Interbreeding $Sox2^{+/cre}$ $E2f7^{+/-}E2f8^{+/-}$ mice with $E2f7^{loxP\ /loxP}E2f8^{loxP\ /loxP}$ mice was sufficient to reconstitute physiologically normal placentas to E2f7-8 deficient fetuses. Yolk sac and placentas from all embryos were taken for PCR analyses to inquire genotypic segregation and to

detect deletion efficiencies in fetuses and placenta. By Taking such genetic approach, I could show that *Sox2*$^{+/cre}$ *E2f7*$^{-/loxp}$ *E2f8*$^{-/loxp}$ pups were born at birth according to Mendalian ratios (Table 4), indicating the vital function of E2f7 and E2f8 in extra-embryonic lineages for embryonic development. To reconfirm that the loss of E2F7 and E2F8 in placenta is the compulsory event to produce mid-gestation death, I again took the advantages of Cre-loxP transgenic system recently established by Pam Wenzel and the Leone lab, which drives Cre-recombinase expression under the control of human Cyp-19 promoter. I bred *Cyp19*$^{+/cre}$ *E2f7*$^{loxp/loxp}$*E2f8*$^{loxp/loxp}$ mice to *E2f7*$^{loxP/loxP}$*E2f8*$^{loxP/loxP}$ mice. Such tissue specific promoter can target expression of Cre-recombinase to the placenta compartment of the embryo exclusively, and thus combining wild-type fetuses with *E2f7* and *E2f8* deficient placenta. *Cyp19*$^{+/cre}$ *E2f7*$^{loxp/loxp}$*E2f8*$^{loxp/loxp}$ embryos were developmentally retarded (significantly smaller fetus size) at E9.5; they progressively began to demonstrate dilated vessels specifically in and around umbilical cord, mimicking the observed phenotype of *E2f7* and *E2f8* null embryos. Finally, embryos of above genotype died and absorbed at E11.5 and no *Cyp19*$^{+/cre}$ *E2f7*$^{loxp/loxp}$ *E2f8*$^{loxp/loxp}$ embryos were found from that stage on (Table 5). This finding presented that disruption of *E2f7* and *E2f8* in extra-embryonic compartment alone can command lethality. Furthermore, this suggests that the apoptotic and hemorrhaging phenotypes seen in the fetal tissues of *E2f7-8* null embryos might have been a secondary result to the extra-embryonic pressure of losing *E2f7* and *E2f8*.

E2F7 and E2F8 can complex to Rb or its pocket proteins

The resemblance of *E2f7* and *E2f8* deficient animals to Rb-null animals directed me to further explore the relationship between pRb and E2F7 or E2F8, to observe if there exits any physical interaction. Due to the limitation of immunoprecipitation-quality antibody for both

E2F7 and E2F8, I utilized over-expression of plasmids containing epitope-tags to complete the co-immunoprecipitation procedures described here. In a series of transfections and co-immunoprecipitations, E2F7 was found to physically interacting to pRb, p130 and p107, detected by immunoblotting techniques (Figure 11a, 11c, 11e). However, under a similar experimental design, E2F8 showed no detectable association with pRb, p130 and p107 (Figure 11b, 11d, 11f). Since it was shown that E2F7 and E2F8 can form hetero-dimer (Figure 3), it is conceivable that E2F8 might still be in complex with Rb through its binding to E2F7.

I also explored that E2F7 and E2F8 might also be associated with other co-repressors with co-. Thus, I performed similar co-immunoprecipitations, transfecting epitope-tagged E2F7 or E2F8 and differentially tagged co-repressor candidates, such as HDACs and Sin3s. Upon co-immunoprecipitation, I identified that E2F7 and E2F8 both present physical interactions to HDAC1 (Figure 12a and 12b) and Sin3a (Figure 12b and 12d). This finding supplemented the association of Rb to E2F7 and E2F8 in that E2F8 can complex to Rb through the association to E2F7 or the association to groups of co-repressors.

Discussion

The E2F7 and E2F8 transcription factors were the final members of the E2F family to be identified. Here I show that unlike the function of other E2Fs, E2F7 and E2F8 are strictly required for embryonic development. Their combined loss resulted in the accumulation of *E2f1* and *p53*, widespread apoptosis, vascular defects and embryonic death by E11.5. The targeted inactivation of *E2f1* or *p53* suppressed the apoptosis in DKO embryos, suggesting that E2F7 and E2F8 control apoptosis via the E2F1-p53 axis. The importance of E2F7 and E2F8 in embryonic development was shown to be specifically confined to the extra-embryonic cell lineages.

Phenotypes of developmental defects due to the ablation of *E2f7* and *E2f8* largely resembled the physiological responses to losing a closely related molecular partner, Rb, and this has led us to hypothesize that E2F7 and E2F8 are the direct mediator of Rb function.

E2F7 and E2F8 constitute a distinct arm of the E2F network

Because of the intense interest in E2Fs as major regulators of the cell cycle and apoptosis, individual E2F family members, including *E2f1* through *E2f6*, have been extensively studied *in vivo* by gene targeting approaches in mice. With the exception of *E2f3* knockout mice, the specific defects that have been described for embryos deficient in each of the known E2Fs are rather subtle (Field et al., 1996; Yamasaki et al., 1996; Murga et al., 2001; Zhu et al., 2001). Disruption of the *E2f3* gene in a mixed genetic background yields viable mice (Humboldt et al, 2000; Wu et al 2001), whereas its disruption in pure strains results in embryonic lethality at around E12.5 (GL, unpublished observation). It is surprising that embryos deficient for each of these E2Fs, even those deficient for *E2f3*, have no or little apparent defect in cellular proliferation and apoptosis. This virtual absence of cell proliferation and apoptotic phenotypes in these knockout embryos has raised the possibility that E2Fs are either not critical for the control of proliferation and apoptosis *in vivo* or that there is sufficient functional redundancy among family members to accommodate for a deficiency in any single E2F.

The role of E2F7 and E2F8 in mouse development was investigated here. The targeted disruption of *E2f7* and *E2f8* had little consequence on development; however, their combined ablation resulted in widespread apoptosis, vascular defects and hemorrhaging, leading to embryonic death by E11.5. Provision of even one functional allele from either *loci* was sufficient to carry fetuses through development all the way to birth. E2F7 and E2F8 can form

homodimers and heterodimers. Homodimerization of E2F8 when E2F7 is absent, and vice versa, may provide a molecular explanation for their functional redundancy during embryonic development.

The contribution of E2F7 and E2F8, however, towards postnatal development does not appear to be equal. Young and adult *E2f7*$^{+/-}$*E2f8*$^{-/-}$ mice were of normal size and appeared developmentally normal, but most *E2f7*$^{-/-}$*E2f8*$^{+/-}$ animals were runted and died within their first month of life (C.R. and J.L., unpublished results). A bias in homo- versus hetero-dimerization may explain the differential requirement for *E2f7* and *E2f8* in adult development. I found that in tissue culture experiments at least, under conditions where expression levels can be compared (by epitope tagging) and experimentally equalized, the formation of E2F7:E2F7 homodimers was preferred over E2F7:E2F8 heterodimers; E2F8:E2F8 homodimers appeared to be the least preferred state (E2F7:E2F7 > E2F7:E2F8 >E2F8:E2F8). While the molecular basis for homo- versus hetero-dimerization is not yet clear, these data suggest that inefficient homodimerization may compromise the ability of E2F8 to compensate for the loss of *E2f7*, an effect that might be aggravated in circumstances of limiting amounts of E2F8 (*E2f7*$^{-/-}$*E2f8*$^{+/-}$). Thus, the observed bias for E2F7 homodimerization may explain the stricter postnatal requirement for this subunit. While this interpretation is likely an oversimplification, these results do provide a molecular explanation for their functional redundancy in development. It will be interesting to investigate how dimerization might be impacted by the levels of E2F7 and E2F8 proteins *in vivo* or by tissue-specific signals.

E2F7 and E2F8 regulate S-G_2 specific expression of E2F-dependent genes.

E2F7 and E2F8 may have a particularly important role in repressing E2F-targets as cells transit through S phase. Gene expression analysis in synchronized *E2f7*$^{-/-}$*E2f8*$^{-/-}$ MEFs revealed that *E2f1* mRNA levels, as well as that of many other E2F-target genes, increased acutely during S and G_2. This E2F7 and E2F8-mediated repression coincided with the time in the cell cycle at which *E2f7* and *E2f8* levels peak (de Bruin et al; Maiti et al). Why the expression of E2F-targets need to be kept low during S and G_2 is not entirely clear, but at least three mechanisms have evolved to achieve this. One mechanism involves the binding of cyclin A/cdk2 to E2F1, E2F2 and E2F3a during S phase, leading to the phosphorylation of the dimerization partner DP1/2 and the inhibition of E2F/DP DNA binding activity. A second mechanism involves the Skp2/F-box-dependent degradation of the three E2F activators during S phase (Leone et al, 1998). Both the binding of cyclin A/cdk2 and the Skp2-dependent degradation of E2F activators require conserved domains within their N-termini. Here I describe a third mechanism that involves E2F7- and E2F8-mediated repression of target genes that include the *E2f1* and *E2f3a* genes themselves, ensuring that E2F-targets are kept at the lowest possible levels during S and G_2. Thus, E2F7 and E2F8 appear to have a distinct role from the other E2F repressors (E2F3b, E2F4, E2F5 and E2F6), which play a more acute role in G_0-G_1, by participating in transcription repression during S-G_2. By directly regulating the expression of *E2f1* and *E2f3a*, E2F7 and E2F8 couple S/G_2 transitions to the control of G_0/G_1.

E2F7 and E2F8 regulate apoptosis via the E2F1-p53 axis.

In vitro and *in vivo* experiments described here provide clear-cut evidence in support of a role for E2F7 and E2F8 in the control of apoptosis. The mechanism of their action involves, at least in part, the regulation of *E2f1* expression. ChIP experiments showed that E2F7 and E2F8 are

recruited to the *E2f1* promoter. Consistent with a role in repression of *E2f1*, genetic inactivation of *E2f7* and *E2f8* resulted in the accumulation of *E2f1* mRNA and a corresponding increase in its protein product. *E2f1* promoter reporter assays indicated that the basis for the accumulation of *E2f1* mRNA in *E2f7*$^{-/-}$*E2f8*$^{-/-}$ cells likely involves a transcriptional mechanism. Together, these results demonstrate a direct role for E2F7 and E2F8 in the repression of *E2f1*.

The increase in *E2f1* protein levels in *E2f7*$^{-/-}$*E2f8*$^{-/-}$ cells coincided with the accumulation of p53 protein. Several mechanisms of how E2F1 may lead to the accumulation and activation of p53 have been described. For example, E2F1 overexpression has been shown to induce the expression of *p19*^{ARF} . A key function of p19^{ARF} protein is to bind and sequester MDM2 to the nucleolus, and thereby prevent the MDM2-mediated degradation of p53 (Bates et al. 1998). E2F1 can also induce the expression of the ATM and CHK2 kinases, resulting in the phosphorylation, accumulation and activation of p53 (Russell et al. 2002; Rogoff et al. 2002). Moreover, E2F1 interacts directly with p53 via its N-terminal cyclin A binding domain, and this interaction enhances the apoptotic activity of p53 (Hsieh et al. 2002). Hence, the accumulation of E2F1 protein can lead, via a number of mechanisms, to an increase of p53 protein and activity.

The accumulation of E2F1 and p53 in *E2f7*$^{-/-}$*E2f8*$^{-/-}$ cells is of physiological significance since ablation of either *E2f1* or *p53* suppressed the widespread apoptosis observed in DKO embryos. Clearly, E2F7 and E2F8 are likely involved in repressing many more targets than just *E2f1*, and so it is not surprising that loss of *E2f1* or *p53* did not suppress the embryonic lethality phenotype. These latter results suggest that apoptosis in *E2f7*$^{-/-}$*E2f8*$^{-/-}$ embryos is not simply due to an indirect consequence of perturbed signaling associated with embryonic lethality, but rather a specific signal emanating from E2F1. Consistent with this interpretation, the conditional ablation of *E2f7* and *E2f8* sensitized MEFs to apoptotic signals, suggesting that this susceptibility

involves a cell autonomous mechanism. Together, these data show that E2F7 and E2F8 form an essential arm of the E2F network involved in the control of apoptosis via the E2F1-p53 axis.

Functions and Characteristics of E2F7 and E2F8 revealed them as potential mediators of Rb

The *E2f7* and *E2f8* genes are essential in maintaining normal in embryonic development; at least one functional allele is required for the viability of offspring fetuses. *E2f7* and *E2f8* deficient embryos showed severe vasculature defects and ectopic apoptosis as a result to up-regulation of E2F1 and p53. The phenotypic response to the simultaneous deletion of *E2f7* and *E2f8* during embryo development was significantly more severe than that found in of E2F knock-out models. These phenotypes were intriguingly similar to $Rb^{-/-}$ embryonic phenotype. Specifically the apoptotic phenotypes were in both cases via activation of E2F1 and p53 (de Bruin A.. et al, 2003). The ectopic E2F1 and p53 expression suggests that the regulation of apoptosis, at least under cytotoxic pressure, Rb and E2f7-8 are involved in the regulation of the *E2f1-p53* axis (Harbour and Dean, 2000).

Among other physiological defects of the mid-term lethality of *E2f7* and *E2f8* deficient embryos, *E2f7* and *E2f8*'s biological function in constructing the placental-fetal interfaces was a particularly important event in ensuring embryonic survival. Using Cre-loxP approaches to reconstitute functional placentas in E2f7-8 deficient embryos, I could show that the lethal phenotypes were suppressed allowing *E2f7-8* deficient pups deliver at almost normal mendalian ratios. Furthermore, specific ablation of *E2f7* and *E2f8* in extra-embryonic tissue could mimic the $E2f7^{-/-}E2f8^{-/-}$ embryonic phenotypes including the early lethality, supporting the idea that loss of *E2f7* and *E2f8* in extra-embryonic lineages is the compulsory event for the observed lethality.

The finding was striking similarity to the extra-embryonic function of Rb in mid-stages of embryonic development (Wu et al, 2002). Later in post-partum murine development, the physiological effect of losing *E2f7* and *E2f8* continues to resemble that of Rb. Specially, *E2f7* and *E2f8* deficient animals that were delivered by supplying the wild-type placentas also encounter neonatal deaths.

The speculation that E2F7 and E2F8 are potential mediators of Rb function was investigated by analyzing the possibility of physical interactions between Rb, its pocket proteins and *E2f7* or *E2f8*. I found that E2F7 was capable of binding to all three Rb family members to other know transcriptional co-repressors. These binding activities could provide a reasonable explanation of the discrepancies that I observed between E2F7-8 mutant embryos and Rb mutant embryos ($E2f7^{-/-}E2f8^{-/-}$ embryo died at E11.5 and $Rb^{-/-}$ died at E14.5), since p130 and p107 could potentially compensate for the loss of Rb. E2F8 was found to be less tightly related to Rb, in which no direct association was found. However, its recruitment to other co-repressors and its hetero dimer-partner E2F7 granted E2F8 the capacity to reside in the Rb-E2F7-E2F8 complex (data not shown).

In summary, E2F7 and E2F8 are essential for embryonic development and may be viewed as a distinct arm of the E2F network that is involved in mediating Rb function. I demonstrate that *E2f1* represents a particularly critical target that if not tightly repressed by E2F7 and E2F8 can elicit widespread apoptosis in developing embryos.

Acknowledgement

I would like to thank Jing Li, who helped in all stages of this project in both planning of experiments and in actual execution of the project. I would like to thank Gustavo Leone for his guidance and for providing the project with financial support. I would like to thank Anthony Trimboli for his help on various staining protocols. I would like to thank the rest of the Leone lab for technical advice and support during this project.

References:

1. Attwooll C., Lazzerini D. E., and Helin K. 2004.. The E2f family: the specific functions and overlapping interests. *Embo J*. **23:**4709-4716.
2. Bates S., Phillips A.C., Clark P.A., Stott F., Peters G., Ludwig R.L., and Vousden K.H. 1998. p14ARF links the tumour suppressors RB and p53. *Nature*. **395:** 124-125.
3. Bell L.A., and Ryan K.M. 2004. Life and death decisions by E2F-1. *Cell Death Differ*. **11:** 137-42.
4. Christensen J., Cloos P., Toftegaard U., Klinkenberg D., Bracken A.P., Trinh E., Heeran M., Di Stefano L., and Helin K. 2005. Characterization of E2F8, a novel E2F-like cell-cycle regulated repressor of E2F-activated transcription. *Nucleic Acids Res.* **33:** 5458-5470.
5. de Bruin A., Maiti B., Jakoi L., Timmers C., Buerki R., and Leone G. 2003. Identification and characterization of E2F7, a novel mammalian E2F family member capable of blocking cellular proliferation. *J Biol Chem.* **278:** 42041-42049.

6. de Bruin A., Wu L., Saavedra H. I., Wilson P., Yang Y., Thomas R. J, Weinstein M., Robison M.L., and Leone G. Rb function in extraembryonic lineages suppresses apoptosis in the CNS of Rb-deficient mice. *Proc Natl Acad Sci U S A.* **11:** 6546-6551.

7. Di Stefano L., Jensen M.R., and Helin K. 2003. E2F7, a novel E2F featuring DP-independent repression of a subset of E2F-regulated genes. *EMBO J.* **22:** 6289-6298.

8. Dimova D.K., and Dyson N.J. 2005. The E2F transcriptional network: old acquaintances with new faces. *Oncogene.* **24:** 2810-2826

9. Field S.J., Tsai F.Y., Kuo F., Zubiaga A.M., Kaelin W.G. Jr., Livingston D.M, Orkin SH., and Greenberg M.E. 1996. E2F-1 functions in mice to promote apoptosis and suppress proliferation. *Cell.* **85:** 549-561.

10. Grana X., Garriga J. and Mayo X. 1998 Role of the retinoblastoma protein family, pRB, p107 and P130 in the negative control of cell growth. *Oncogene*. **17**: 3365-3383.

11. Harbour J. W., and Dean D. C. 2000. *Genes Dev.* **14:** 2393-2409.

12. Hsieh J.K., Yap D., O'Connor D.J., Fogal V., Fallis L., Chan F., Zhong S., and Lu X. 2002. Novel function of the cyclin A binding site of E2F in regulating p53-induced apoptosis in response to DNA damage. *Mol Cell Biol.* **22:** 78-93.

13. Humbert P.O., Rogers C., Ganiatsas S., Landsberg R.L., Trimarchi J.M., Dandapani S., Brugnara C., Erdman S., Schrenzel M., Bronson R.T., and Lees J.A. 2000. E2F4 is essential for normal erythrocyte maturation and neonatal viability. *Mol Cell.* **6:** 281-291.

14. Humbert P.O., Verona R., Trimarchi J.M., Rogers C., Dandapani S., amd Lees J.A. 2000. E2f3 is critical for normal cellular proliferation. *Genes Dev.* **14:** 690-703.

15. Kamijo T., Weber J.D., Zambetti G., Zindy F., Roussel M.F., and Sherr C.J. 1998. Functional and physical interactions of the ARF tumor suppressor with p53 and Mdm2. *Proc Natl Acad Sci U S A.* **95:** 8292-8297.

16. Leone G., DeGregori J., Yan Z., Jakoi L., Ishida S., Williams R.S., and Nevins J.R. 1998. E2F3 activity is regulated during the cell cycle and is required for the induction of S phase. *Genes Dev.* **12:** 2120-2130.

17. Logan N., Delavaine L., Graham A., Reilly C., Wilson J., Brummelkamp T.R., Hijmans E.M., Bernards R., and La Thangue N.B. 2004. E2F-7: a distinctive E2F family member with an unusual organization of DNA-binding domains. *Oncogene.* **23:** 5138-5150.

18. Logan N., Graham A., Zhao X., Fisher R., Maiti B., Leone G., and La Thangue N.B. 2005. E2F-8: an E2F family member with a similar organization of DNA-binding domains to E2F-7. *Oncogene.* **24:** 5000-5004.

19. Wenzel P. L., Wu L., Chong L., Chen W., Dureska G., Sites E., Pan T., Sharma A., Huang K., Ridgeway R., Mosaliganti K., Sharp R., Machiraju R., Saltz J., Yamamoto H., Cross J.C., Roberson M.L., Leone G. 2007. Rb is critical in a mammalian tissue stem cell population. *Genes Dev.* **21:** 85-97.

20. Wu L., de Bruin A., Saavedra H.I., Starovic M., Trimboli A., Yang Y., Opavska J., Wilson P., Thompson J.C., Ostrowstki M. C., Thomas, J. R., Woollett L.A., Weinstein M., Cross J. C., Robinson M.L., and Leone G. 2003. *Nature.* **427**: 942-947.

21. Yamasaki L., Jacks T., Bronson R., Goillot E., Harlow E., and Dyson N.J. 1996. Tumor induction and tissue atrophy in mice lacking E2F-1. *Cell.* **85:** 537-548.

22. Zhu J.W., Field S.J., Gore L., Thompson M., Yang H., Fujiwara Y., Cardiff R.D., Greenberg M., Orkin S.H., and DeGregori J. 2001. E2F1 and E2F2 determine thresholds

for antigen-induced T-cell proliferation and suppress tumorigenesis. *Mol Cell Biol.* **21:** 8547-8564.

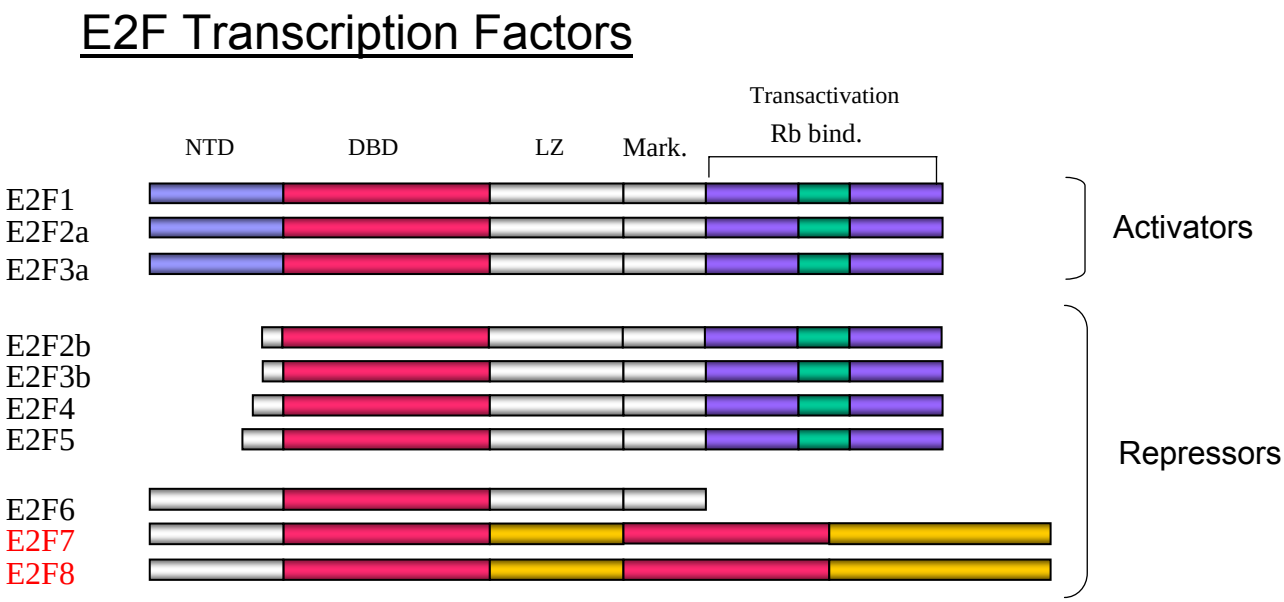

Figure 1. Schematic representations of E2F transcription factors. Eight distinct E2F gene loci encode for ten different E2F isoforms. A conserved DNA binding domain (DBD) is the feature that distinguishes each isoform as a member of the E2F family of transcription factors. The N-terminal domain (NTD) of E2F1-3 harbors the cyclin A-binding and Skp-binding domains and is distinct from the NTD of E2F6-8. The leuzine zipper (LZ) domain common to E2F1-6 is involved in dimerizing with DP1 or DP2, but is absent in E2F7-8. The Marked (Mark.) domain common to E2F1-6 is involved in mediating interactions with co-factors; The classical Rb binding (Rb bind.) domain buried within the activation domain is common to E2F1-5.

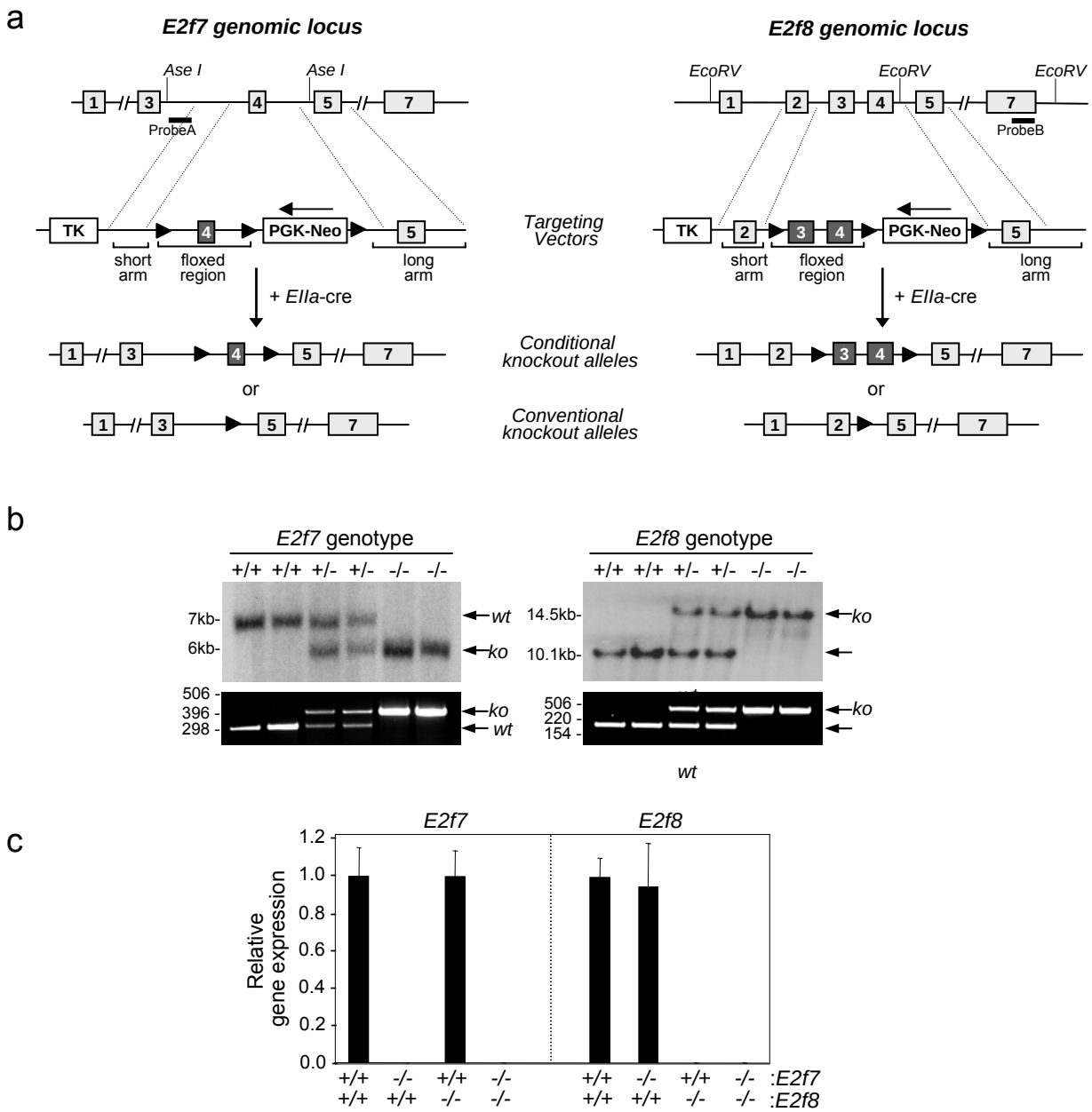

Figure 2. Generation of *E2f7* and *E2f8* knockout mice. (**a**) Targeting strategies of *E2f7* (left) and *E2f8* (right) knockout mice. Upper: partial exon/intron structures of the *E2f7* and *E2f8* genes. The black bars under genomic sequence indicate the position of probes used for Southern analysis. Middle: the targeting vectors, positions of TK and Neo (rectangle), as well as loxP sites (filled triangles) are indicated. Bottom two: predicted conditional or conventional homologous recombination events. **(b)** Southern analysis of genomic DNA isolated from conventional knockout mice tails digested with Ase I for *E2f7*(left) and EcoR V for *E2f8* (right) and hybridized using probes A or B, respectively (top). Genotyping of tail DNA was performed using allele specific PCR primers described in Methods (bottom). **(c)** Real-time RT-PCR analysis of *E2f7* or *E2f8* transcript using primers located in the knockout region. Results are average ± SD of embryo cDNA samples in triplicate. The genotypes are indicated at the bottom.

TABLE 1: Genotypic analysis of embryos during development

	E2f7$^{+/+}$			*E2f7*$^{+/-}$			*E2f7*$^{-/-}$			total
	E2f8$^{+/+}$	*E2f8*$^{+/-}$	*E2f8*$^{-/-}$	*E2f8*$^{+/+}$	*E2f8*$^{+/-}$	*E2f8*$^{-/-}$	*E2f8*$^{+/+}$	*E2f8*$^{+/-}$	*E2f8*$^{-/-}$	
E9.5	6	16	29	16	72(2)	53(1)	12	58(1)	33	299
expected	*5*	*28*	*22*	*19*	*75*	*56*	*13*	*47*	*34*	
E10.5	9	21	13	7(1)	45	28(1)	4(1)	28(1)	6(7)[a]	172
expected	*7*	*20*	*13*	*16*	*43*	*28*	*8*	*23*	*14*	
E11.5	-	6	4	2	15(2)	14(2)	2(1)	8(1)	0(5)[b]	62
expected	*-*	*5*	*5*	*3*	*16*	*13*	*3*	*10*	*8*	
E12.5	-	-	3	-	4	17(2)	-	3	0(9)[b]	38
expected	*-*	*-*	*5*	*-*	*4*	*15*	*-*	*4*	*10*	
P0	7	22	16	24	45	17	5	18	0[b]	154
expected	*8*	*18*	*10*	*18*	*39*	*21*	*10*	*21*	*11*	

() number of dead embryos; Exact binomial test: [a] significant ($p<0.0015$), [b] highly significant ($p<0.0007$).

Table 1. Genotypic analysis of *E2f7* and *E2f8* double knockout embryos survival at the indicated stages of development.

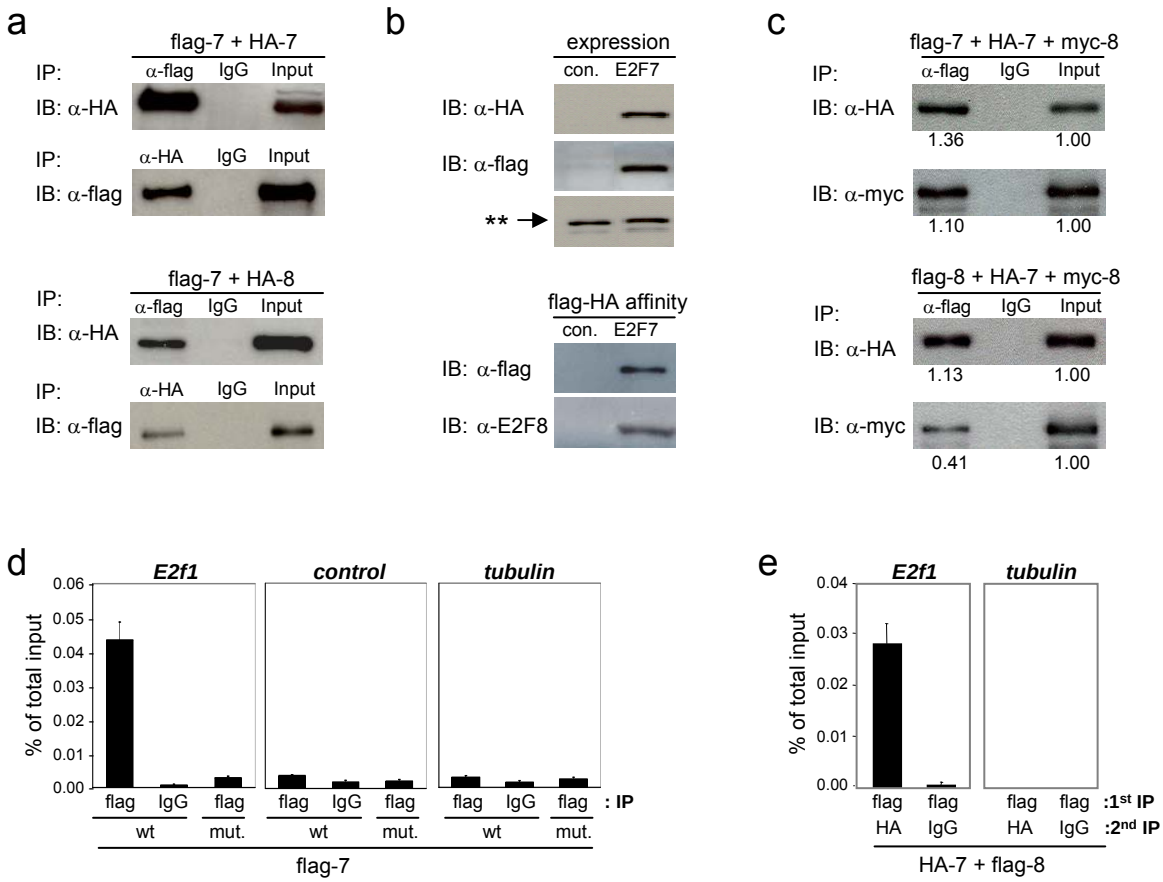

Figure 3. E2F7 and E2F8 homo- and hetero-dimerize and bind to *E2f1* promoter. (**a**) Lysates from HEK293 cells transfected with both flag-tagged and HA-tagged E2F7 and E2F8 were co-immunoprecipitated (IP) with anti-flag antibody and immunoblotted (IB) with anti-HA antibody or *vice versa*. Immunoprecipitation with normal mouse IgG was used as a negative IP control to rule out nonspecific bindings. (**b**) Upper panels: stable expression of flag-HA-E2F7 in Hela cells. After sorting, flag-HA-E2F7 transduced Hela cells were harvested and subjected to Western blot to test the ectopic E2F7 expression by using flag and HA specific antibodies. Non-specific band from HA block was used as a loading control. Bottom panels: E2F8 was identified from E2F7 complex purification. Nuclear extracts from flag-HA-7 expressing cells were immunoprecipitated with flag antibody affinity resins. Western blots were performed by using antibody against endogenous E2F8. Mock-transduced Hela cells were used as a negative control. **(c)** Binding preference of E2F7 and E2F8 was E2F7:E2F7> E2F7: E2F8 > E2F8 : E2F8. Lyaste over-expressing differentially tagged E2F7 and E2F8 was harvested post transfection. Immunoprecipitation of HA-tagged E2F7 (upper panel) and HA-tagged E2F8 (bottom panel) was detected by anti-myc antibody The intensity of signals was measured by densitometer. **(d)** E2F7 binds to the *E2f1* promoter. Chromatin from HEK293 cells overexpressing *wild type* flag-7 (wt) or flag-7DBD1,2 (mut) was immunoprecipitated with anti-flag antibody or normal mouse IgG control. Chromatin immunoprecipitated DNA were specifically amplified by using primers flanking the *E2f1* promoter region with the E2F binding sites, *E2f1* exon1 region (control), and the *tubulin* promoter region. Real-time PCR was performed in triplicate and cycle numbers were normalized to the 1% input. **(e)** E2F7 and E2F8 occupy the *E2f1* promoter simultaneously. HEK293 cells expressing ectopic HA-7 and flag-8 were used and sequential ChIP assay was performed as described in Methods. DNAs collected after two rounds of chromatin immnuoprecipitations as indicated were subjected to real-time PCR analysis to assess the enrichment of the *E2f1* promoter. The *tubulin* promoter was used as a negative promoter control.

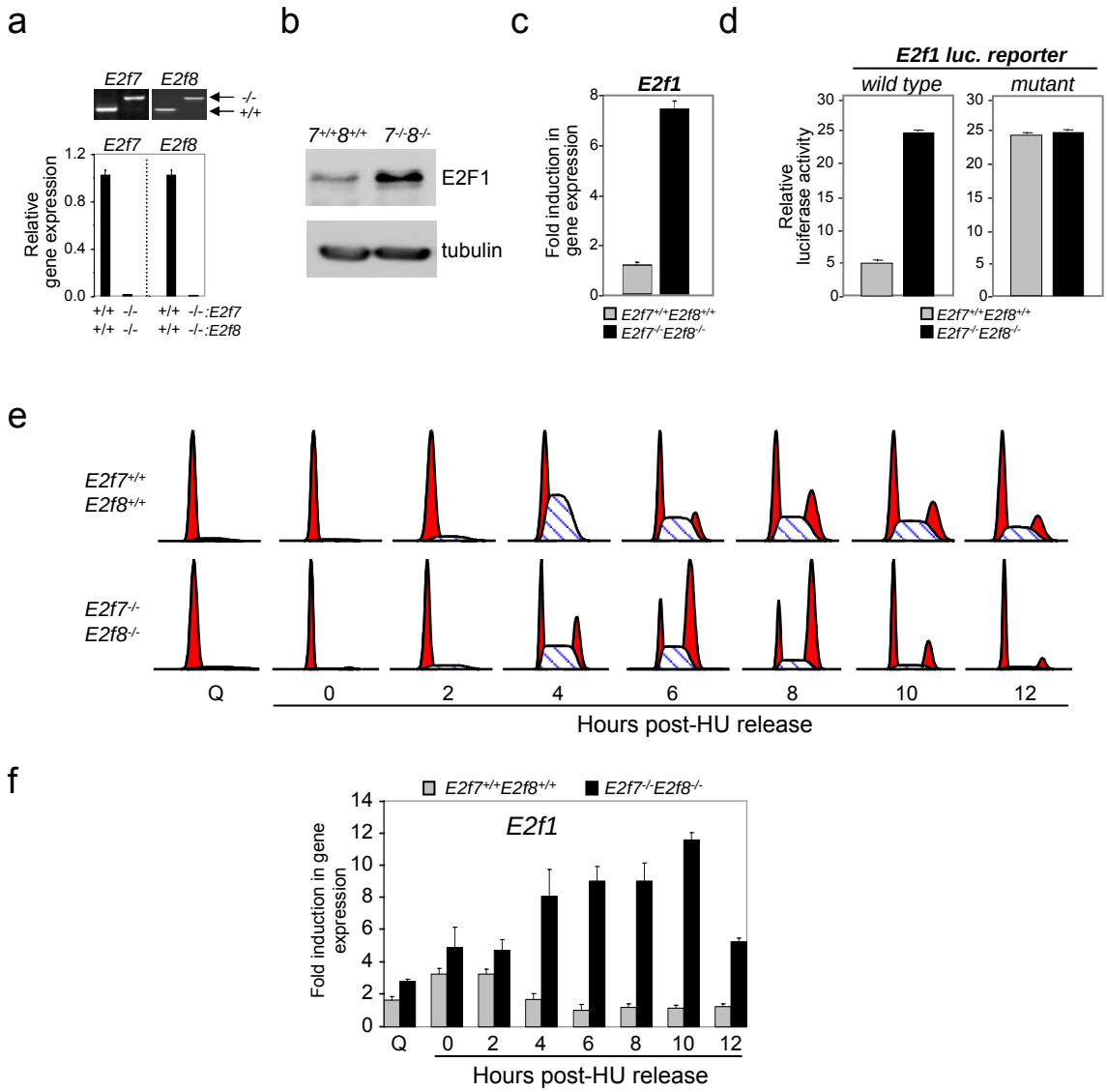

Figure 4. *E2f1* is a direct target of E2F7 and E2F8. **(a)** *E2f7* and *E2f8* expression in MEFs co-respond with their genotypic indication. Upper panel: PCR was performed from cell lysates to confirm the genotypic expression. Bottom panel: Q-PCR was performed to detection of *E2f7* and *E2f8* expression pattern. (**b**) Western blot analysis of lysates from primary MEFs and their *wild type* littermate control. Antibodies specific against E2F1 and p53 were used to test endogenous E2F1 and p53 protein level. (**c**) Expression of *E2f1* in the same MEFs cells were measured by real-time RT-PCR. (**d**) Wild type and *E2f7*$^{-/-}$*E2f8*$^{-/-}$ MEFs were transfected with indicated firefly luciferase reporter plasmids along with thymidine kinase renilla luciferase construct (internal control). Cells were forced into quiescence by serum withdrawal and restimulated with serum to allow cell cycle entry. Cells were harvested at indicated time points and reporter activity was detected using dual luciferase assay system. Reporter luciferase activity was normalized to renilla luciferase and relative luciferase activity is shown in the graph. (**e**) FACS analysis of MEFs with indicated genotypes. MEFs were synchronized by serum starvation and hydroxyurea (HU) block, and then released into the cell cycle. As indicated time points, cells were harvested and stained by propidium iodide for flow cytometry. Q: quiescence. (**f**) Total RNAs were harvested at quiescence or indicated intervals following HU release and subjected to reverse transcription and real-time PCR to analyze relative RNA level of *E2f1.* (**g**) Cell lysates were harvested at quiescence or indicated intervals following HU release and subjected to Western blot to analyze E2F1 protein level. Tubulin was used as a loading control.

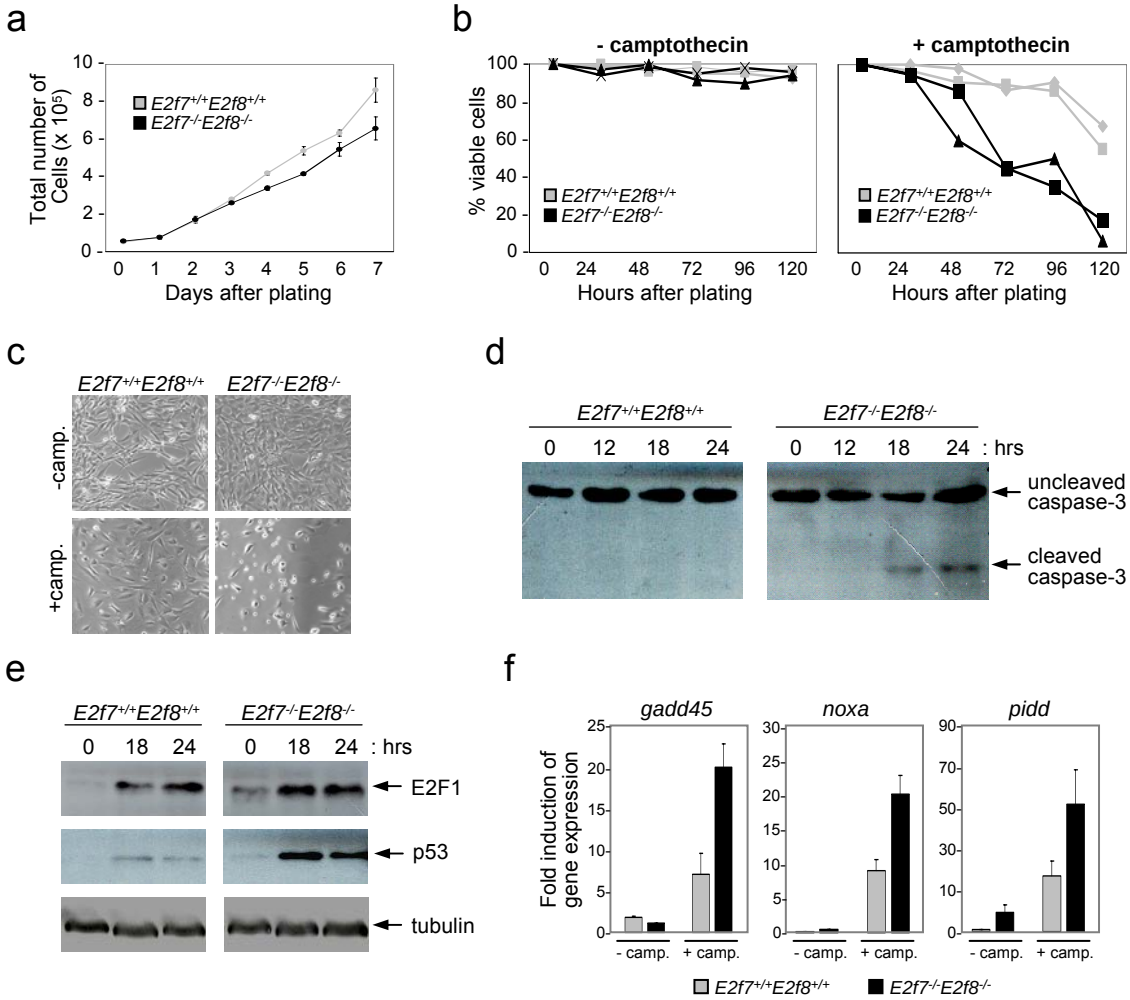

Figure 5. *E2f7* and *E2f8* deficient MEFs are hypersensitive to DNA damage induced apoptosis. (**a**) *E2f7-/-E2f8-/-* has no defect in cellular proliferation. Growth curve analysis of primary MEFs with the indicated genotypes. (**b**) Camptothecin induces more cell death in *E2f7* and *E2f8* deficient MEFs. *Wild type* and *E2f7-/-E2f8-/-* MEFs were mock treated with DMSO (left) or 20μm camptothecin (right) for 18h. At the indicated intervals up to 120h, cells were harvested and viability was determined by trypan blue exclusion. (**c**) Light microscopy images of MEFs with indicated genotyping at 54h after 20μm camptothecin or mock treatment. (**d**) Cisplatin triggers Caspase-3 activation in *E2f7-/-E2f8-/-* MEFs but not in the *wild type* control. MEFs with indicated genotypes were treated with 10μm cisplatin for 24h. Lysates were analyzed at the indicated time points by Western blot for Caspase-3 cleavage. (**e**) Western analysis of E2F1 and p53 proteins expression in the indicated cells after 18h and 24h of 20μm camptothecin treatment. Tubulin was detected as an internal control. (**f**) Total RNA was extracted from cells with indicated genotypes after 18h camptothecin treatment. Expression of indicated p53-target genes were measured by real-time RT-PCR. Results are shown as fold induction in triplicate.

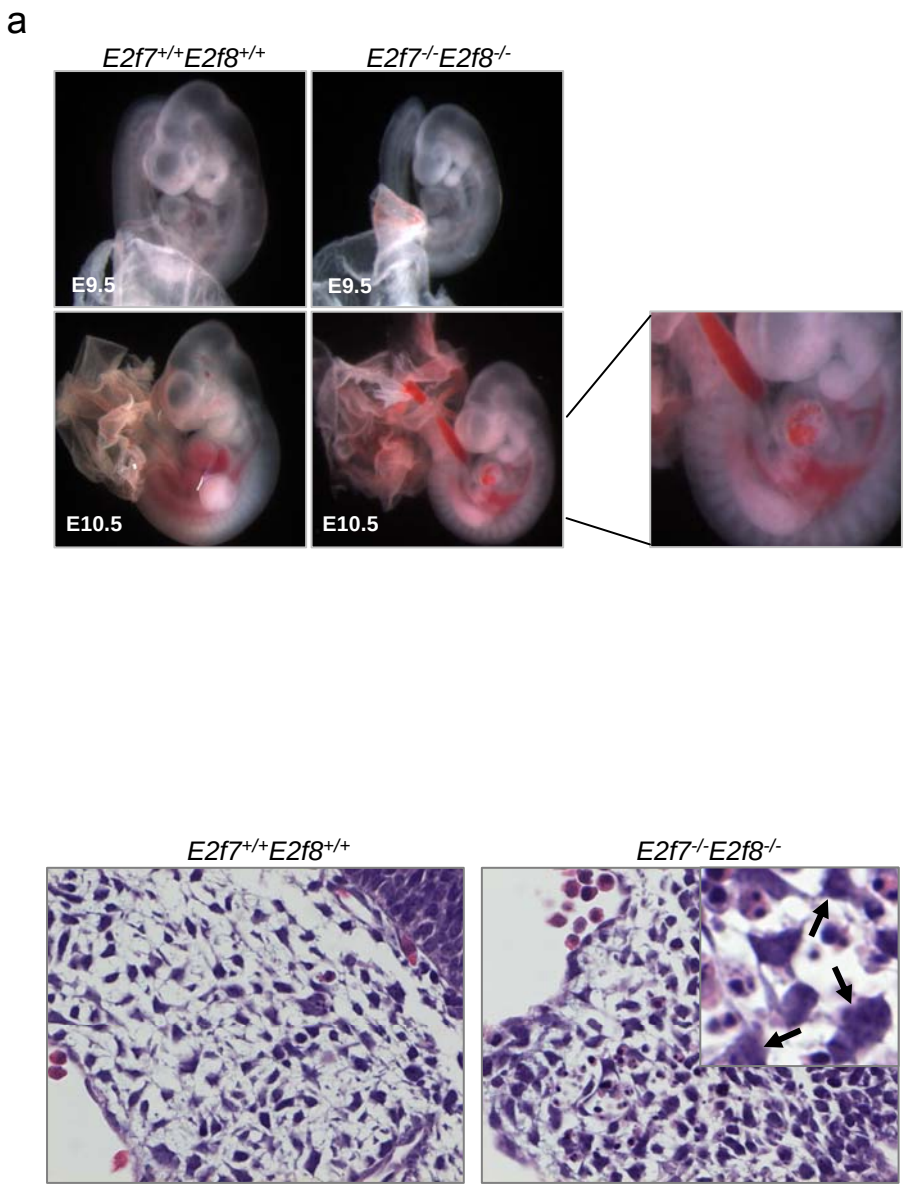

Figure 6. *E2f7* and *E2f8* deficient embryos showed angiogenesis defect. (a) Gross view of embryos at E9.5 and E10.5 days of embryonic development. Images were taken at 16x magnification using light microscope. (**b**) HE staining of E9.5 embryos.

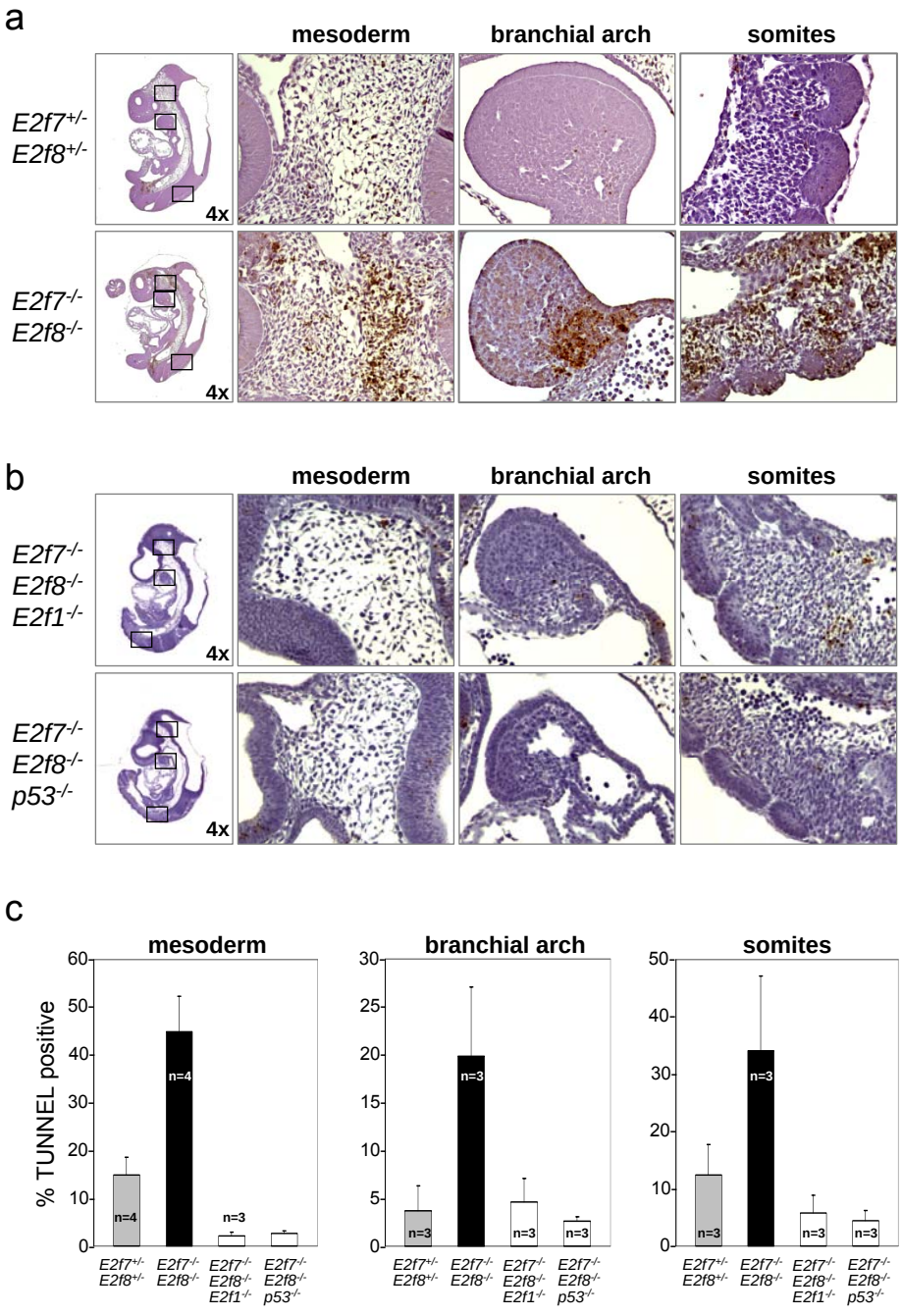

Figure 7. *E2f7* and *E2f8* deficient embryos show increased apoptosis *in vivo* at E9.5. (**a**) Cell death of embryos with the indicated genotypes was assessed by TUNEL assay using 5μm formalin fixed paraffin sections. Most left: low magnification pictures of the whole embryos. Right three: high magnification pictures of the boxed areas from the low magnification pictures. (**b)** TUNEL staining of *E2f1*$^{-/-}$*E2f7*$^{-/-}$*E2f8*$^{-/-}$ triple knockout embryos (top), and *p53*$^{-/-}$*E2f7*$^{-/-}$*E2f8*$^{-/-}$ triple knockout embryos (bottom). (**c)** Quantification of apoptosis of the indicated tissue areas as determined by TUNEL assay. Results are average ± SD of the percentage of total number of cells that are TUNEL-positive. At least 3 different embryos were counted for each genotyping group.

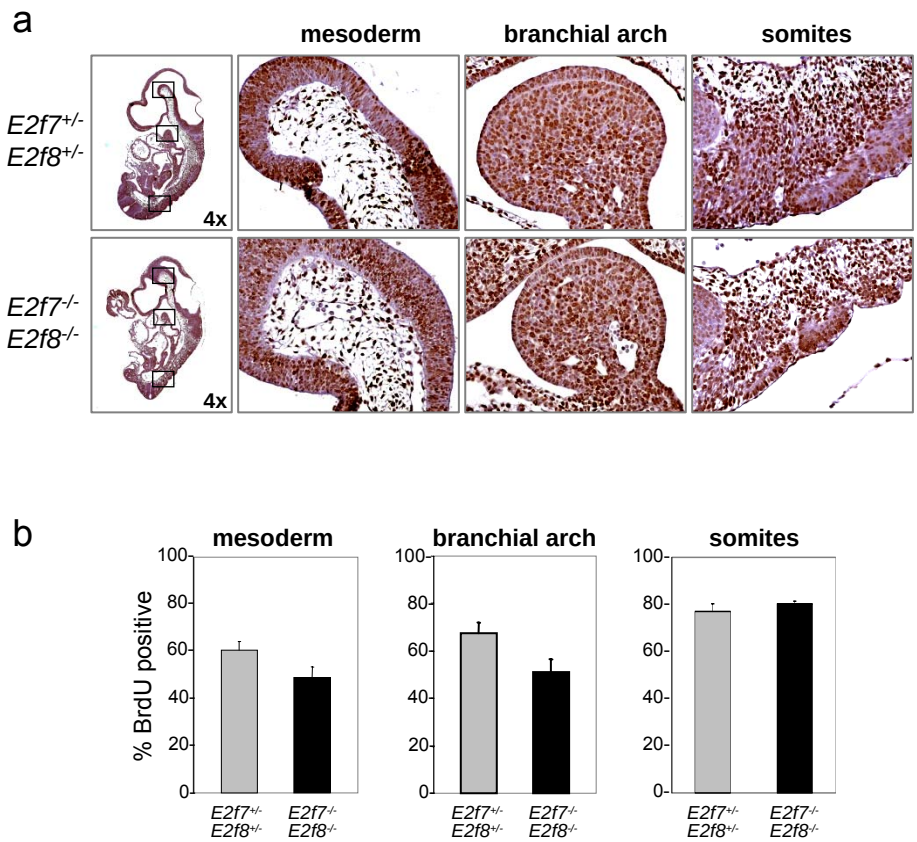

Figure 8. Inactivation of *E2f7* and *E2f8* has no effect on proliferation *in vivo* at E9.5. (**a**) BrdU staining of embryos with indicated genotypes. Most left: low magnification pictures of the whole embryos. Right three: high magnification pictures of the boxed areas from the low magnification pictures. (**b)** Proliferation indexes of different tissue areas with indicated genotypes were quantified by the percentage of total number of cells that are BrdU-positive.

TABLE 2: Genotypic analysis of embryos during development

	E2f1$^{+/+}$ / *E2f7*$^{-/-}$*E2f8*$^{-/-}$	*E2f1*$^{+/-}$ / *E2f7*$^{-/-}$*E2f8*$^{-/-}$	*E2f1*$^{-/-}$ / *E2f7*$^{-/-}$*E2f8*$^{-/-}$	total
E9.5	-	2	5	46
expected	*-*	*5*	*6*	
E12.5	-	-	0(4)[a]	10
expected	*-*	*-*	*3*	

() number of dead embryos; Exact binomial test: [a] highly significant ($p<0.0007$)

Table 2. Genotypic analysis of *E2f1*, *E2f7* and *E2f8* triple knockout embryos survival at the indicated stages of development.

TABLE 3: Genotypic analysis of embryos during development

	$p53^{+/+}$ $E2f7^{-/-}E2f8^{-/-}$	$p53^{+/-}$ $E2f7^{-/-}E2f8^{-/-}$	$p53^{-/-}$ $E2f7^{-/-}E2f8^{-/-}$	total
E9.5	3	6	4	66
expected	*4*	*8*	*4*	
E12.5	0	0(1)	0(4)[a]	12
expected	*1*	*2*	*1*	

() number of dead embryos; Exact binomial test: [a] highly significant ($p<0.0007$).

Table 3. Genotypic analysis of *p53, E2f7; E2f8* Triple knock-out embryo survival at indicated stages of development.

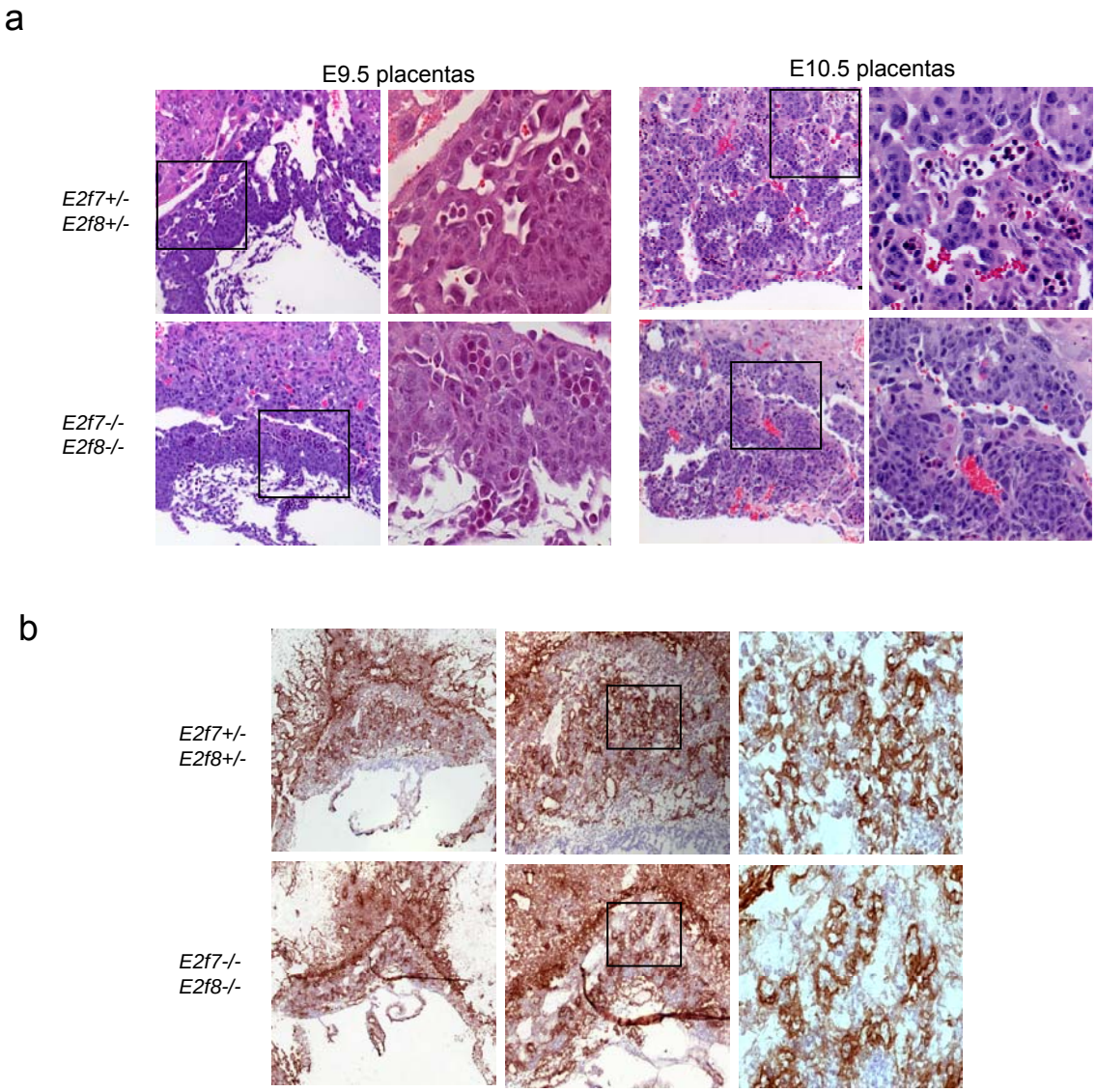

Figure 9. Extra-embryonic function of E2f7 and E2f8 are essential for embryonic development. E2F7 and E2F8 disruption causes vascular defect in the labyrinth layer of the placenta. (**a-b**) placentas have marked defects in placental vascularization. (**a**) Hematoxylin and eosin staining of placentas of E10.5 wild-type verse *E2f7*$^{-/-}$*E2f8*$^{-/-}$ embryos. cp, chorionic plate; lb, labyrinth layer; m, maternal blood cells; f, fetal blood cells (nucleated). (**b**) Immunostaining for PECAM-1 (brown) on sections from E10.5 wild-type and E2F7 and E2F8 null placentas at E10.5. Faint nuclear counterstaining (blue) was achieved with Meyer's hematoxylin.

TABLE 4: Genotypic analysis of embryos during development: Sox2-Cre Deletion

		E2f7$^{-/loxp}$		*E2f7*$^{+/loxp}$		*CreE2f7*$^{-/loxp}$		*CreE2f7*$^{+/loxp}$	
	total	*E2f8*$^{-/loxp}$	*E2f8*$^{+/loxp}$	*E2f8*$^{-/loxp}$	*E2f8*$^{+/loxp}$	*E2f8*$^{-/loxp}$	*E2f8*$^{+/loxp}$	*E2f8*$^{-/loxp}$	*E2f8*$^{+/loxp}$
E10.5	28	4	--	5	--	4	--	5	--
expected		*3*	--	*3*	--	*3*	--	*3*	--
E12.5	27	1	--	7	--	2	--	4	--
expected		*3*	--	*3*	--	*3*	--	*3*	--
P0	33	3	4	6	5	3	6	3	3
expected		*4*	*4*	*4*	*4*	*4*	*4*	*4*	*4*

Table 4. Genotypic analysis of genetic rescue from interbreeding Sox-2 Cre animals to *E2f7 E2f8* conventional deletion animals

TABLE 5: Genotypic analysis of embryos during development: Cyp19-Cre Deletion

		E2f7$^{-/loxp}$		*E2f7*$^{+/loxp}$		*CreE2f7*$^{-/loxp}$		*CreE2f7*$^{+/loxp}$	
	total	*E2f8*$^{-/loxp}$	*E2f8*$^{+/loxp}$	*E2f8*$^{-/loxp}$	*E2f8*$^{+/loxp}$	*E2f8*$^{-/loxp}$	*E2f8*$^{+/loxp}$	*E2f8*$^{-/loxp}$	*E2f8*$^{+/loxp}$
E10.5	13	2	1	0	1	0(3)[a]	--	1	5
expected		*1*	*1*	*1*	*2*	*1*	*1*	*1*	*1*
E12.5	20	4	3	5	1	0(2)[a]	3	1	3
expected		*2*	*2*	*2*	*2*	*2*	*2*	*2*	*2*

() number of dead embryos; Exact binomial test: [a] significant ($p<0.05$).

Table 5. Genotypic analysis of genetic rescue from interbreeding Cyp-19 Cre animals to *E2f7 E2f8* conventional deletion animals.

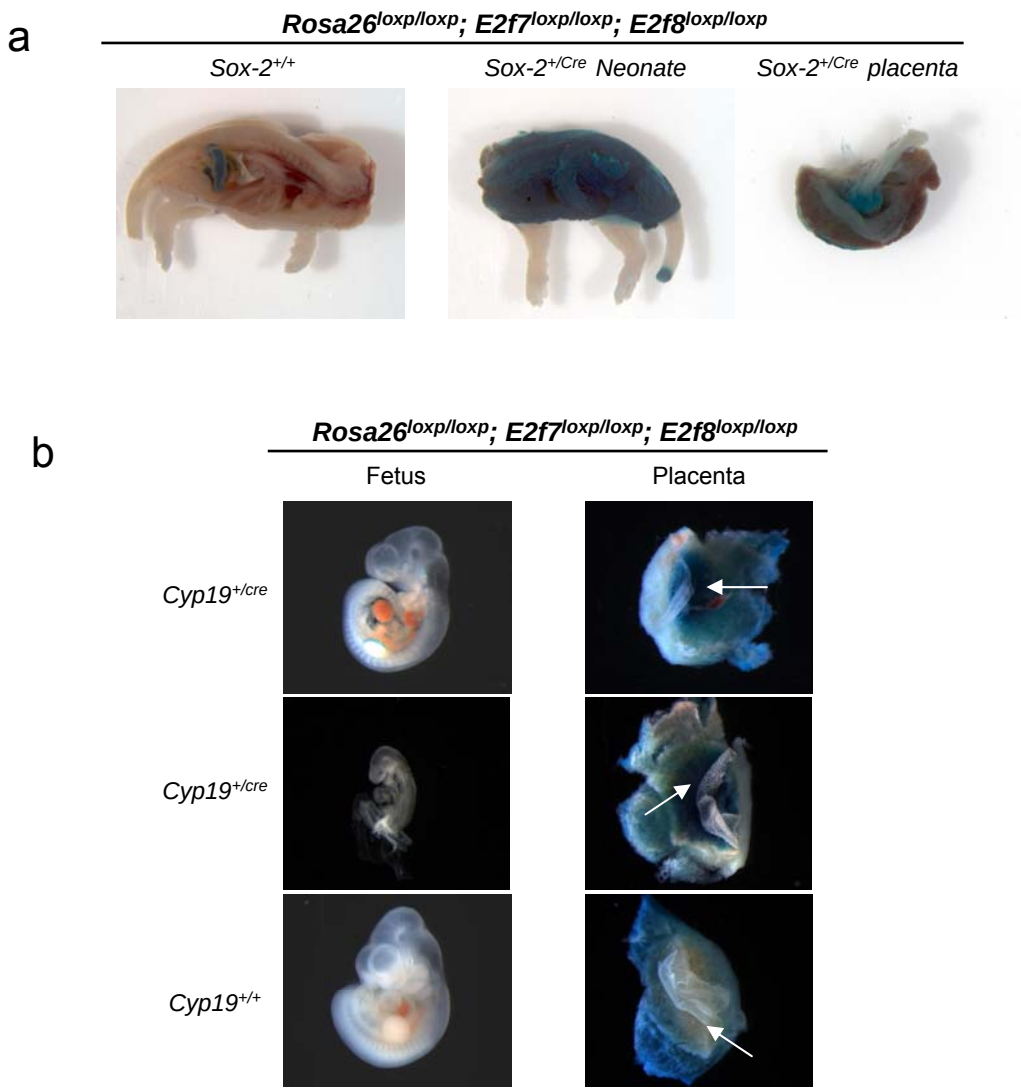

Figure 10. Endogenous promoter Sox-2 and Cyp-19 can direct specific Cre-recombinase expression in desired tissue types. **(a)** B-galactosidase analysis of *Sox-2$^{+/Cre}$ E2f7$^{loxp/loxp}$ E2f8$^{loxp/loxp}$* P0 neonates and its placenta in comparison to wild-type neonates. **(b)** B-galactosidase analysis of *Sox-2$^{+/Cre}$ E2f7$^{loxp/loxp}$ E2f8$^{loxp/loxp}$* E12.5 fetuses and their placenta in comparison to wild-type embryos. Enzyme activity will be detected when a dark blue color is observed, which in turn represents the presence of cre expression.

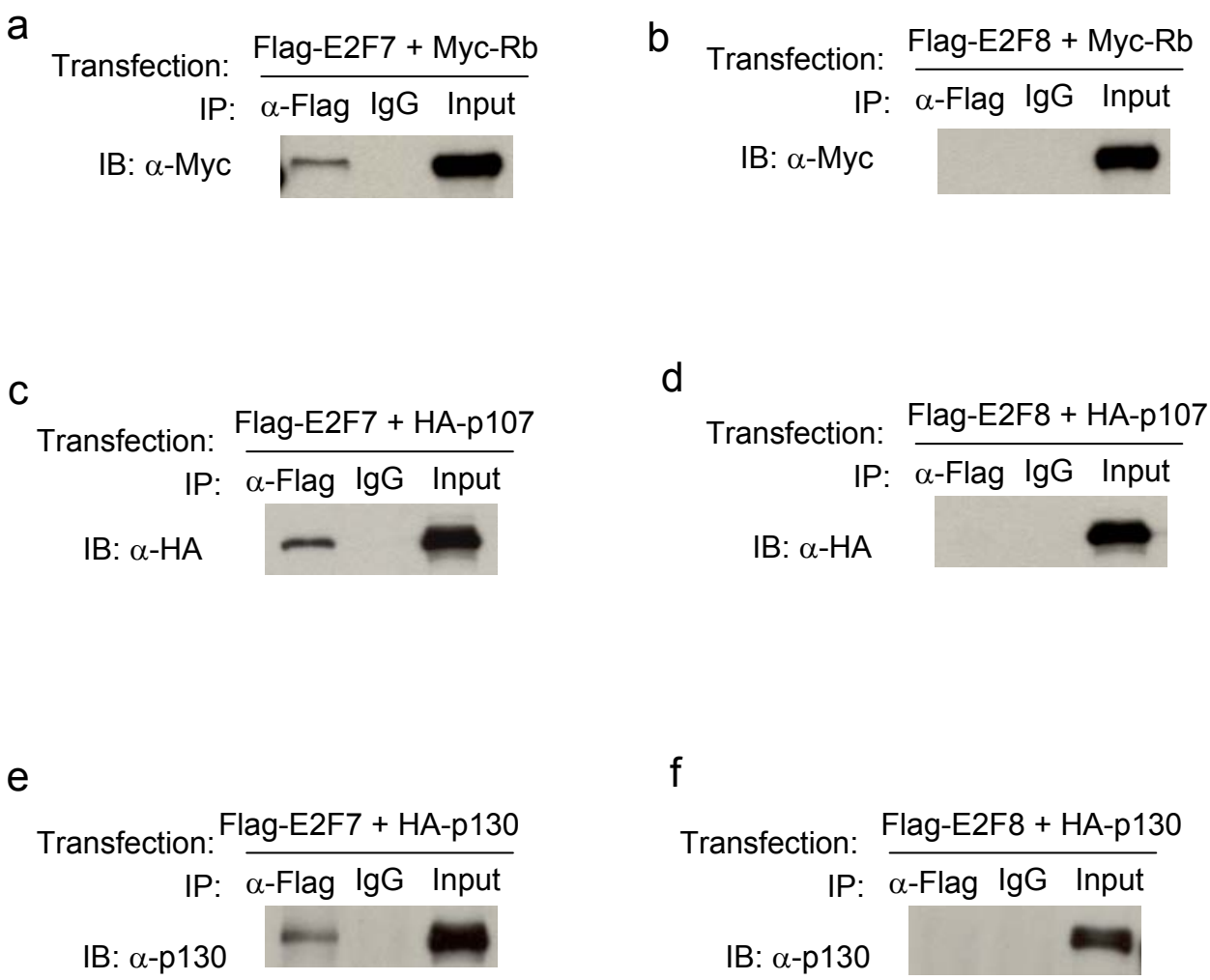

Figure 11. E2F7 and E2F8 associate with Rb and its pocket protein.. Lysates from HEK293 cells transfected with indicated epitope-tagged plasmid were co-immunoprecipitated (IP) with anti-flag antibody and immunoblotted (IB) with anti-myc or anti-HA antibodies. Immunoprecipitation with normal mouse IgG was used as an internal negative control to rule out non-specific bindings **(a)** Flag-tagged E2f7 and myc-tagged Rb **(b)** Flag-tagged E2f8 and myc-tagged Rb **(c)** Flag-tagged E2f7 and HA-tagged p130 **(d)** Flag-tagged E2f8 and HA-tagged p130 **(e)** Flag-tagged E2f7 and HA-tagged p107 **(f)** Flag-tagged E2f7 and HA-tagged p107. All results indicating physical interaction between E2f7 and Rb or its family pocket proteins, but E2F8 fails to show bindings with all three protein in over-expression.

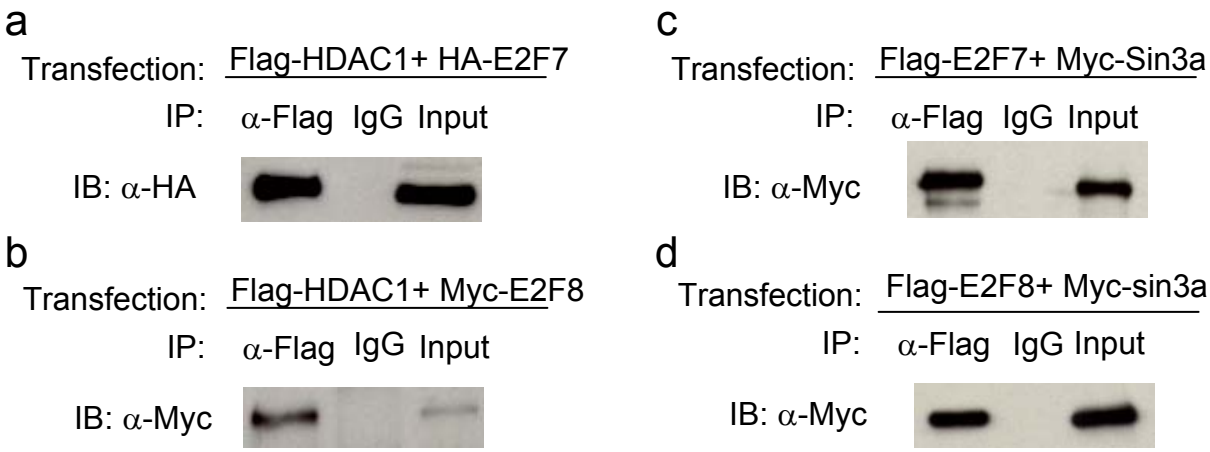

Figure 12. E2F7 and E2F8 can recruit corepressors. Lysates over-expressing (a) Flag-tagged HDAC1 and HA- tagged E2F7; (b) Flag-tagged HDAC1 and HA- tagged E2F8; (c) Flag-tagged E2F7 and myc-tagged Sin3a; (d) Flag-tagged E2F8 and myc-tagged Sin3a were used in co-immunoprecipitation using anti-flag antibody and immunoblotted with anti-HA or anti- myc antibodies. Physical associations were seen among all proteins.